

การดูดซับและการแพร่ของแก๊สดีโมเลกุลในซีโอไลติกอิมิตาโซเลตเฟรมเวิร์ค-90 โดยการจำลองทาง  
คอมพิวเตอร์

นางสาวเฟื่อง หุย โว



จุฬาลงกรณ์มหาวิทยาลัย  
CHULALONGKORN UNIVERSITY

บทคัดย่อและแฟ้มข้อมูลฉบับเต็มของวิทยานิพนธ์ตั้งแต่ปีการศึกษา 2554 ที่ให้บริการในคลังปัญญาจุฬาฯ (CUIR)

เป็นแฟ้มข้อมูลของนิสิตเจ้าของวิทยานิพนธ์ ที่ส่งผ่านทางบัณฑิตวิทยาลัย

วิทยานิพนธ์นี้เป็นส่วนหนึ่งของการศึกษาตามหลักสูตรปริญญาวิทยาศาสตรมหาบัณฑิต

The abstract and full text of theses from the academic year 2011 in Chulalongkorn University Intellectual Repository (CUIR)  
สาขาวิชาเคมี ภาควิชาเคมี  
are the thesis authors' files submitted through the University Graduate School.

คณะวิทยาศาสตร์ จุฬาลงกรณ์มหาวิทยาลัย

ปีการศึกษา 2558

ลิขสิทธิ์ของจุฬาลงกรณ์มหาวิทยาลัย

ADSORPTION AND DIFFUSION OF GUEST MOLECULES IN ZEOLITIC IMIDAZOLATE  
FRAMEWORK-90 BY COMPUTER SIMULATIONS

Miss Phuong Thuy Vo



A Thesis Submitted in Partial Fulfillment of the Requirements  
for the Degree of Master of Science Program in Chemistry

Department of Chemistry

Faculty of Science

Chulalongkorn University

Academic Year 2015

Copyright of Chulalongkorn University

|                   |  |
|-------------------|--|
| Thesis Title      | ADSORPTION AND DIFFUSION OF GUEST<br>MOLECULES IN ZEOLITIC IMIDAZOLATE<br>FRAMEWORK-90 BY COMPUTER SIMULATIONS |
| By                | Miss Phuong Thuy Vo  |
| Field of Study    | Chemistry  |
| Thesis Advisor    | Professor Supot Hannongbua, Ph.D.  |
| Thesis Co-Advisor | Thanyada Rungrotmongkol, Ph.D.<br>Tatiya Chokbunpiam, Ph.D.  |

---

Accepted by the Faculty of Science, Chulalongkorn University in Partial  
Fulfillment of the Requirements for the Master's Degree

.....Dean of the Faculty of Science  
(Associate Professor Polkit Sangvanich, Ph.D.)

THESIS COMMITTEE

.....Chairman  
(Associate Professor Vudhichai Parasuk, Ph.D.)

.....Thesis Advisor  
(Professor Supot Hannongbua, Ph.D.)

.....Thesis Co-Advisor  
(Thanyada Rungrotmongkol, Ph.D.)

.....Thesis Co-Advisor  
(Tatiya Chokbunpiam, Ph.D.)

.....Examiner  
(Associate Professor Viwat Vchirawongkwin, Ph.D.)

.....External Examiner  
(Assistant Professor Tawun Remsungnen, Ph.D.)

เฟื่อง ทุย โว : การดูดซับและการแพร่ของแก๊สดีโมเลกุลในซีโอไลติกอิมิดาโซเลตเฟรมเวิร์ค-90 โดยการจำลองทางคอมพิวเตอร์ (ADSORPTION AND DIFFUSION OF GUEST MOLECULES IN ZEOLITIC IMIDAZOLATE FRAMEWORK-90 BY COMPUTER SIMULATIONS) อ.ที่ปรึกษาวิทยานิพนธ์หลัก: ศ. ดร.สุพจน์ หารหนองบัว, อ.ที่ปรึกษาวิทยานิพนธ์ร่วม: ดร.ธัญญา รุ่งโรจน์มงคล, ดร.ตติยา โชคบุญเปี่ยม, 65 หน้า.

วัสดุพรุนโครงข่ายซีโอไลติกอิมิดาโซเลต-90 (ซีฟ-90) ได้รับความสนใจอย่างมากในด้านการคัดแยกก๊าซ เช่น  $\text{CH}_4/\text{H}_2$ ,  $\text{CH}_4/\text{CO}_2$  และ  $\text{CH}_4/\text{N}_2$  เนื่องจากขนาดช่องเปิดของซีฟ-90 จะเป็นเกณฑ์กำหนดสำหรับกระบวนการคัดแยก แต่อย่างไรก็ตามผลจากการทดลองแสดงหลักฐานการดูดซับและการซึมผ่านของก๊าซมีเทนในโครงสร้างซีฟ-90 โดยขนาดเส้นผ่านศูนย์กลางของมีเทนเท่ากับ  $3.8 \text{ \AA}$  ซึ่งใหญ่กว่าขนาดของช่องเปิดของซีฟ-90 ที่มีขนาดเท่ากับ  $3.5 \text{ \AA}$  ที่ได้จากการวัดโครงสร้างซีฟ-90 แบบเชิงเกร็ง ดังนั้นการดูดซับและการแพร่ของมีเทนและไฮโดรเจนในซีฟ-90 ถูกนำมาศึกษาด้วยวิธีพลวัตเชิงโมเลกุลและกิบส์มอนติคาโล อันตรกิริยาหลายชนิดถูกนำมาศึกษาและอันตรกิริยาที่เหมาะสมถูกนำมาใช้ในงานวิจัยนี้ ผลการคำนวณเชิงโครงสร้างและสมบัติไดนามิกส์ของมีเทนและไฮโดรเจนในซีฟ-90 ถูกนำเสนอในงานนี้ โครงสร้างแบบยืดหยุ่นมีอิทธิพลอย่างมากกับการแพร่ ในขณะที่ปริมาณการดูดซับแสดงผลการคำนวณที่ดีในโครงสร้างแบบเชิงเกร็ง ตำแหน่งการดูดซับของแก๊สดีโมเลกุลทั้งสองชนิดคือ มีเทนและไฮโดรเจนถูกพบที่ตำแหน่งโมเลกุลสารอินทรีย์ในโครงสร้างซีฟ-90 นอกจากนี้ผลของประตูเปิดในซีฟ-90 ไม่ถูกพบเมื่อบรรจุโมเลกุลมีเทนและไฮโดรเจนที่ความดันสูงถึง 260 บาร์ จากผลการคำนวณยังแสดงให้เห็นว่าซีฟ-90 เป็นวัสดุที่สามารถคัดแยกก๊าซผสมมีเทนและไฮโดรเจนในอัตราส่วน 1:1 ได้โดยมีค่าประสิทธิภาพการแยกเท่ากับ 4.1

|            |      |                                  |
|------------|------|----------------------------------|
| ภาควิชา    | เคมี | ลายมือชื่อนิสิต .....            |
| สาขาวิชา   | เคมี | ลายมือชื่อ อ.ที่ปรึกษาหลัก ..... |
| ปีการศึกษา | 2558 | ลายมือชื่อ อ.ที่ปรึกษาร่วม ..... |
|            |      | ลายมือชื่อ อ.ที่ปรึกษาร่วม ..... |

# # 5772003823 : MAJOR CHEMISTRY

KEYWORDS: MOLECULAR SIMULATIONS / ADSORPTION / DIFFUSION / CH<sub>4</sub> IN ZIF-90

PHUONG THUY VO: ADSORPTION AND DIFFUSION OF GUEST MOLECULES IN ZEOLITIC IMIDAZOLATE FRAMEWORK-90 BY COMPUTER SIMULATIONS.  
 ADVISOR: PROF. SUPOT HANNONGBUA, Ph.D., CO-ADVISOR: THANYADA RUNGROTMONGKOL, Ph.D., TATIYA CHOKBUNPIAM, Ph.D., 65 pp.

Zeolitic imidazolate framework (ZIF)-90 has interested great consideration in gas separation such as CH<sub>4</sub>/H<sub>2</sub>, CH<sub>4</sub>/CO<sub>2</sub>, CH<sub>4</sub>/N<sub>2</sub> due to its window size that is a factor for separation process. However, there is experimental evidence from adsorption and permeation studies that CH<sub>4</sub> can enter the ZIF-90 framework despite the fact that the critical diameter of CH<sub>4</sub> (3.8 Å) is larger than the window size of ZIF-90 (3.5 Å) assuming a rigid framework. Therefore, adsorption and diffusion of CH<sub>4</sub> and H<sub>2</sub> in the ZIF-90 were investigated by Molecular Dynamics (MD) and Gibbs Ensemble Monte Carlo. Various interaction force fields have been tested and a suitable one has been studied. Results of structural and dynamical properties of CH<sub>4</sub> and H<sub>2</sub> in ZIF-90 are presented in this work. The flexibility has the big influence to the self-diffusion coefficient (Ds) while the good adsorption isotherm can be produced in rigid model. The preferential adsorption site found in RDFs is the organic linker in both guest molecules CH<sub>4</sub> and H<sub>2</sub>. Furthermore, gate opening effect in ZIF-90 was not found in this work when loading CH<sub>4</sub> and H<sub>2</sub> molecules up to a pressure of 260 bar. The results from the mixture CH<sub>4</sub>/H<sub>2</sub> (1:1) show a promising potential of ZIF-90 for gas separation with 4.1 separation factor.

Department: Chemistry

Field of Study: Chemistry

Academic Year: 2015

Student's Signature .....

Advisor's Signature .....

Co-Advisor's Signature .....

Co-Advisor's Signature .....

## ACKNOWLEDGEMENTS

I would like to take this opportunity to express my honest appreciation to all who have helped as well as supported me during two years of my Master thesis.

Firstly, I wish to sincerely thank my advisor-Professor Dr. Supot Hannongbua and my coadvisors – Dr. Thanyada Rungrotmongkol and Dr. Tatiya Chokbunpiam for giving me a great chance to study at Chulalongkorn University as well as all advices and helps without any hesitation. Special thanks to Dr. Tatiya Chokbunpiam for her encouragement to cheer me up during my study.

I also grateful acknowledge Priv-Doz. Dr. Siegfried Fritzsche for all of his suggestions and instructions. I have learned from him not only knowledge but also the way of thinking to be an independent researcher in the future.

I would like to thank Associate Professor Dr. Vudhichai Parasuk, Associate Professor Dr. Viwat Vchirawongkwin and Assistant Professor Dr. Tawun Remsungnen who are not only my thesis committee but also teach me the chemistry background or give me some suggestions for my work.

I wish to express my thanks to my family, all CCUC members for their encouragement and other supports during the time that I stayed in Thailand as a second home.

During my study, I am a student under Scholarship for International graduate students in ASEAN Countries supported by Graduate school, Chulalongkorn University. The Computational Chemistry Unit Cell (CCUC) at Department of Chemistry, Faculty of Science, Chulalongkorn University and the computer center of Leipzig University are acknowledged for computer resources and other facilities.

## CONTENTS

|  | Page |
|--|------|
| THAI ABSTRACT .....                                  | iv   |
| ENGLISH ABSTRACT .....                               | v    |
| ACKNOWLEDGEMENTS .....                               | vi   |
| CONTENTS .....                                       | vii  |
| LIST OF TABLES .....                                 | x    |
| LIST OF FIGURES .....                                | xi   |
| CHAPTER I.....                                       | 1    |
| INTRODUCTION.....                                    | 1    |
| 1.1. Rationale .....                                 | 1    |
| 1.2. Zeolitic Imidazolate Framework-90 (ZIF-90)..... | 4    |
| 1.3. Application.....                                | 5    |
| 1.3.1. Catalyst .....                                | 5    |
| 1.3.2. Drug delivery.....                            | 6    |
| 1.3.3. Sensor.....                                   | 6    |
| 1.3.4. Gas storage.....                              | 6    |
| 1.3.5. Gas and biofuel separation.....               | 6    |
| 1.4. Literature review.....                          | 7    |
| 1.5. Scope of research .....                         | 10   |
| CHAPTER 2.....                                       | 12   |
| THEORY BACKGROUND .....                              | 12   |
| 2.1. Simulation techniques .....                     | 12   |
| 2.1.1. Force field parameters .....                  | 12   |

|  | Page |
|--|------|
| 2.1.2. Periodic boundary conditions .....  | 14   |
| 2.1.3. Ensembles .....   | 16   |
| 2.1.4. Radial distribution functions (RDFs).....   | 16   |
| 2.2. Gibbs Ensemble Monte Carlo simulation (GEMC).....   | 18   |
| 2.3. Molecular dynamics simulation (MD simulation) .....   | 19   |
| 2.3.1. Classical mechanics .....   | 19   |
| 2.3.2. Algorithm .....   | 22   |
| 2.4. Gas transport.....  | 23   |
| 2.4.1. Mechanism of gas transport .....  | 23   |
| 2.4.2. Diffusion, Adsorption and Permeability.....   | 24   |
| CHAPTER III .....  | 27   |
| CALCULATION DETAILS .....  | 27   |
| 3.1. Model and force field parameters.....   | 27   |
| 3.2. Gibbs Ensemble Monte Carlo simulations (GEMC).....  | 29   |
| 3.3. Molecular Dynamics simulations (MD).....  | 31   |
| CHAPTER IV .....   | 33   |
| RESULTS AND DISCUSSION.....  | 33   |
| 4.1. Methane in ZIF-90.....  | 33   |
| 4.1.1 Test of different force fields for the simulation of adsorption isotherm<br>and the structure of ZIF-90..... | 33   |
| 4.1.2. Static properties .....   | 37   |
| 4.1.3. Adsorption sites.....   | 40   |
| 4.1.4. Dynamical properties .....  | 43   |



|   | Page |
|---|------|
| 4.2. Hydrogen.....  | 46   |
| 4.2.1. Adsorption and the preferential adsorption site of hydrogen and<br>mixture in ZIF-90 ..... | 46   |
| 4.2.2. Diffusion and membrane selectivity.....  | 48   |
| CHAPTER V .....   | 51   |
| CONCLUSION .....  | 51   |
| REFERENCES .....  | 52   |
| VITA.....   | 65   |



## LIST OF TABLES

|  |    |
|--|----|
| Table 3.1. Partial charges of the atoms in the ZIF-90 framework (the name of atom type can be found at figure S1 in the appendix)..... | 27 |
| Table 3.2. Force fields for methane.....   | 29 |
| Table 4.1. The box length distribution that was obtained from NPT ensemble MD....  | 36 |
| Table 4.2. Comparison of window sizes of ZIF-90 from different force fields with the experiment.....                                   | 37 |



## LIST OF FIGURES

|  |    |
|--|----|
| Figure 1.1. The bridging angles in metal IMs (1) and zeolites.....   | 4  |
| Figure 1.2. The structure of Zeolitic Imidazolate Framework-90.....  | 4  |
| Figure 2.1. The bonded potential; a) bond stretching potential, b) angle bending potential, c) torsion angle potential.....  | 12 |
| Figure 2.2. The van der Waals potential between two particles.....   | 14 |
| Figure 2.3. Periodic boundary condition.....   | 15 |
| Figure 2.4. The radial distribution function (RDF).....  | 17 |
| Figure 2.5. The radial distribution function for a simple fluid.....   | 17 |
| Figure 2.6. The possible movement in Gibb Ensemble Monte Carlo.....  | 18 |
| Figure 2.7. The different numerical approximations for the slope.....  | 22 |
| Figure 2.8. The mechanism of CH <sub>4</sub> /H <sub>2</sub> transport through a membrane with surface diffusion.....  | 24 |
| Figure 3.1. Structure of ZIF-90. The 6-membered ring is called 'window' (w in the left part of the picture).....   | 27 |
| Figure 4.1. a) Comparison of adsorption isotherms of five force fields for CH <sub>4</sub> (FF1-FF5) in ZIF-90 (GAFF and DREID.) at 303 K, b) the adsorption isotherm of CH <sub>4</sub> in ZIF-90 at 303 K after scaling the force field of the framework. Experimental data from Venkatasubramanian et al..... | 33 |
| Figure 4.2. Adsorption isotherm of CH <sub>4</sub> in ZIF-90 at 303 K for low pressure (0-1.2 bar) obtained from GEMC for the force field with and without modification. Experimental data from Venkatasubramanian et al.....  | 35 |
| Figure 4.3. Distribution of the fluctuating window size of the flexible ZIF-90 framework without guest molecules at 300 K.....   | 37 |
| Figure 4.4. Probability density of CH <sub>4</sub> in (a) rigid model and (b) flexible model at 2.5, 10 and 15 CH <sub>4</sub> molecules/cage.....   | 38 |

|   |    |
|---|----|
| Figure 4.5. RDFs of the interaction between methane-methane and methane-ZIF-90 lattice in GEMC, rigid and flexible MD simulations at very low loading (0.5 CH <sub>4</sub> molecules/cage) with modified GAFF at 300 K..... | 39 |
| Figure 4.6. Uptake of CH <sub>4</sub> by ZIF-90 at 300 K in mmol/g as a function of the chemical potential (kJ/mol) as obtained both from GEMC (MC_rigid) and flexible MD.....  | 41 |
| Figure 4.7. RDF of different atom types in ZIF-90 with CH <sub>4</sub> at loadings of a) 0.5 molecules/cage, b) 15 molecules/cage at 300 K.....   | 41 |
| Fig. 4.8. Adsorption isotherm of CH <sub>4</sub> in ZIF-90 at 300 K for pressures 0-255 bar.....  | 43 |
| Figure 4.9. Comparison of $D_s$ for CH <sub>4</sub> in rigid and flexible ZIF-90 frameworks at 300 K....  | 44 |
| Figure 4.10. Distributions of the window size of ZIF-90 for different loadings of CH <sub>4</sub> at 300 K.....   | 45 |
| Figure 4.11. The adsorption isotherm of methane, hydrogen and mixture CH <sub>4</sub> /H <sub>2</sub> with the ratio 1:1.....   | 46 |
| Figure 4.12. The adsorption selectivities of mixture CH <sub>4</sub> /H <sub>2</sub> with ratio 1:1.....  | 47 |
| Figure 4.13. The RDFs of selected atom types in ZIF-90 with methane (a, c) and hydrogen (b, d) in two different concentrations.....   | 47 |
| Figure 4.14. The self-diffusion coefficient of methane, hydrogen and mixture CH <sub>4</sub> /H <sub>2</sub> with the ratio 1:1.....  | 49 |
| Figure 4.15. Distributions of the window size of ZIF-90 for different loadings of mixture CH <sub>4</sub> /H <sub>2</sub> with ratio 1:1 at 300 K.....  | 49 |
| Figure 4.16. Probability density of mixture CH <sub>4</sub> /H <sub>2</sub> ratio 1:1 in flexible model. The red dots represented H <sub>2</sub> while the green dots represented CH <sub>4</sub> .....                     | 50 |

## CHAPTER I

### INTRODUCTION

#### 1.1. Rationale

Porous materials recently have been an interesting research area. These materials have many benefits in various fields from ion exchange, separation to catalysis. In the past zeolites have been among the most popular materials that were used in many applications in industry such as Zeolite Y, ZSM-5, mordenit, beta. However, the limitation of pore size or flexibility are disadvantages of these materials.

Recently, new porous materials called Metal-Organic Frameworks (MOFs) or well-known with coordination polymer [1] have been found which had many good properties like higher surface area, larger pore volume and adjustable pore size. That's why they have gotten a lot of attention from scientists. MOFs are created by the link between organic units and metal transition and are presumed as promising candidates for many industrial applications.

Especially, a subclass of MOFs which has the zeolitic structure, called Zeolitic Imidazolate Frameworks (ZIFs) has been synthesized. Combing good properties of both MOFs and Zeolite, mentioned before (large surface areas, pore volume), with the exceptional chemical and thermal stability, there is no surprise when ZIFs are emerging in material research in recent years. Until now there are over 150 ZIF structures found by replacing the metal, linker or just the functional groups in linkers [2]. This rapid development of ZIF's shows to some extent the importance of these new materials.

However, some MOFs have pore windows which are too large or too small compared with diameters of gases like CO<sub>2</sub>, CH<sub>4</sub> and N<sub>2</sub>, it may lead to low separation factors in adsorption/desorption of gases. In ZIF-90, the Zn<sup>2+</sup> ions are interconnected by imidazolate-carboxyaldehyde anions to a SOD structure with a pore size of 3.5 Å [3] which is between the molecular size of CO<sub>2</sub> (3.3 Å) and CH<sub>4</sub> (3.8 Å). This pore size of 3.5 Å recommends ZIF-90 as a candidate for the separation of CO<sub>2</sub> from bio or

natural gas by molecular sieving. Further, the aldehyde group of the ZIF-90 linker interacts additionally with CO<sub>2</sub> [4]. However, in adsorption studies also small alcohols with a critical diameter > 4 Å could be adsorbed on ZIF-90 [5] and methane easily permeates through ZIF-90 membranes [6-9].

While adsorption and diffusion of guests in ZIF-8 have been widely studied by different theoretical methods, for ZIF-90 only a few theoretical studies seem to exist.

Atci and Keskin [10] have simulated the adsorption and diffusion of various gases in ZIF-90 and other ZIFs thus evaluating the separation potential of different ZIFs. But, they used the rigid model for all frameworks with the UFF force field of non-bonded interactions. Thornton et al. [11] performed the first simulations on flexible framework of ZIF-90, however, they focused mainly on ZIF-11 and they modified the DREIDING force field to obtain the adsorption isotherms of ZIF-11. Furthermore, the lack of the charges in their model strongly affects the simulations of non-spherical molecules like CO<sub>2</sub> or N<sub>2</sub> with partial charges that result in quadrupole moments. Gee et al. [5] performed in a pioneering paper examinations of the diffusion and adsorption of small alcohols in ZIF-90 in both rigid and flexible models, in which the interactions were described by GAFF and DREIDING force fields. The results showed a significant effect between rigid and flexible framework in the self-diffusion coefficient ( $D_s$ ) and the flexible model using GAFF gives better results compared with the experiment. This influence of the flexibility on  $D_s$  can also be found in other ZIFs [12-14] and MOFs [15] while the adsorption isotherm seems to be much less sensitive with respect to the lattice flexibility [16, 17] as long as no structural phase transition like the so called gate opening [18-20] takes place. On the other hand, Zhang et al. [21] found that the DREIDING force field produced better results than GAFF in terms of the adsorption isotherm. Therefore, the choice of interaction parameters for rigid and flexible models in terms of adsorption isotherms and  $D_s$  and the effect of the gas molecule concentration on the ZIF's structure are still questionable.

Hydrogen (H<sub>2</sub>) is regarded as a future fuel or fuel cell which is clean, renewable and reduces the green-house effect. To produce hydrogen for application, one of the

most popular method is steam reforming and methane ( $\text{CH}_4$ ), well-known for being one of the impurities, needs to be removed or separated from hydrogen. That is also the reason why many researchers try to find materials having a high selectivity for  $\text{CH}_4/\text{H}_2$  mixtures. In addition, methane is the main component of natural gas and of biogas. Before methane is used in many industrial processes and energetically in households and industry, it has to be concentrated; usually  $\text{CO}_2$  and  $\text{N}_2$  have to be separated by using different technologies. Adsorption or permeation using ZIF-90 adsorbents or membranes, respectively, could become novel options. Although having a bigger diameter (3.8 Å) compared with the the window size (the average one in a flexible lattice) of some ZIFs like ZIF-8 (3.4 Å) and ZIF-90 (3.5 Å) [3, 22], methane can diffuse within these frameworks.

In this work, structural properties like density distributions and radial distribution functions (RDFs) as well as adsorption and the dynamics of self-diffusion of methane molecules in ZIF-90 are examined by both Molecular Dynamics (MD) and Gibbs Ensemble Monte Carlo (GEMC) simulations. Studying diffusion and adsorption of methane and hydrogen in ZIF-90 by simulations will investigate the effect of the flexibility of the framework on these properties but, also a possible influence of the adsorbed molecules on the lattice structure *e.g.* gate opening as found in [15, 18, 20] for other MOF's and ZIF's and guest molecules can be checked. In addition, a better understanding on the atomic level for physical processes like the adsorption isotherm, diffusion mechanisms, or adsorption sites can be achieved.

Unfortunately, there is still a lot of uncertainty about the choice of parameters to be used in such simulations. Hence, a part of the examination must be dedicated to the comparison and evaluation of existing force fields. Therefore, in this work, various parameters for the ZIF-90 lattice and for methane molecules from the literature will be tested and compared for rigid and flexible models. The results obtained in this way will hopefully provide parameters yielding good agreement with experiments in terms of adsorption isotherms, X-ray structure and dynamical properties.

## 1.2. Zeolitic Imidazolate Framework-90 (ZIF-90)

Being a subclass of Metal organic frameworks (MOFs), zeolitic imidazolate frameworks (ZIFs) are composed of tetrahedral metal ion (M) and the organic linker that can be imidazolate (Im) or its derivatives. Interestingly, the angle metal-Im-metal in ZIFs is approximate  $145^\circ$ , similar with angle Si-O-Si in zeolites [22]. Due to the zeolite like structure in ZIFs, they possess a higher stability than other MOFs which is useful in the industrial application.

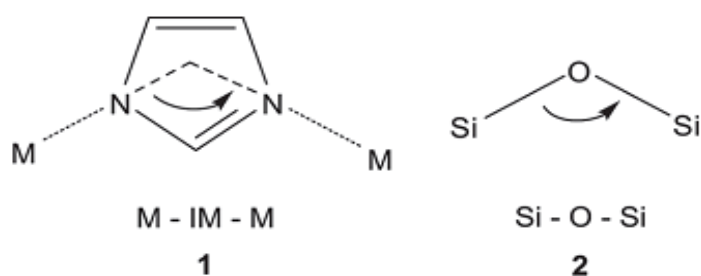


Figure 1.1. The bridging angles in metal IMs (1) and zeolites (2) [22]

ZIF-90 ( $\text{Zn}(\text{C}_4\text{H}_3\text{N}_2\text{O})_2$ ) was synthesized first time in 2008, and is composed of tetrahedral metal ion ( $\text{ZnN}_4$ ) with linker imidazolate-2-carboxyaldehyde (Ica). There are two types of apertures which are composed of four linkers (4-member ring) and six linkers (6-member ring) in figure 2. The largest cavity diameter up to  $11.0 \text{ \AA}$  and window size (6-member ring) is  $3.5 \text{ \AA}$  [3].

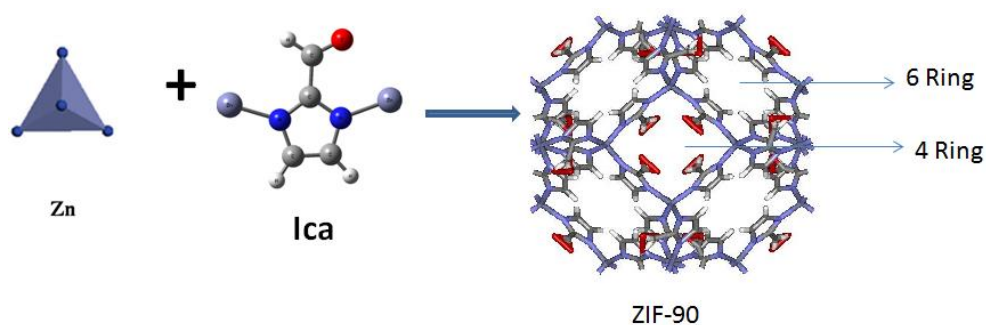


Figure 1.2. The structure of Zeolitic Imidazolate Framework-90

Other thermo- and chemical properties:



- ZIF-90 exhibits an exceptional thermos- and chemical stability, it can be stable even in the range 300-500°C and maintain its structure in water, toluene and methanol for 24 hours with a permanent porosity.
- The Langmuir surface area is 1320 m<sup>2</sup>/g
- Total pore volume is 0.58 (cm<sup>3</sup>.g<sup>-1</sup>)

Obtaining a lot of interesting properties, ZIF-90 exhibits many promising applications in the future for gas separation, gas purification, catalysis.

### 1.3. Application

Based on those above mentioned unique intrinsic properties, ZIFs show the potential in many industry application. For example, the large surface area and high pore volume in some ZIFs are very useful for storing gases or holding nanoparticles in catalysts. The adjustable structure and tunable pore size are exceptional features that are applied in catalyst, sensor or separation processes. In addition, with a higher stability compared with other MOFs, using ZIFs in the industry synthesis processes is much easier and more effective.

#### 1.3.1. Catalyst

Possessing 3D structure with continuous permeable channels and tunable pore size, ZIFs can provide the environment for the catalyst and modify easily the polar-nonpolar, hydrophobic-hydrophilic characterization which is very crucial in bio-reaction or synthesis. Knoevenagel reaction, Friedel-Crafts acylation, hydrogen production, oxidation, epoxidation and so on are some of many examples for using ZIFs like an active catalyst [23].

ZIF-90 was studied to encapsulate gold nano-particles into its cavities and was formed at Au@ZIF-90 nano-composite catalyst in the aerobic oxidation reaction. Due to the functional group, it can stabilize and monodisperse the size-matched Au nano-particles [24].

### 1.3.2. Drug delivery

The large surface area, high pore volume and exceptional thermal and chemical stability are good properties for storing and releasing drugs. Furthermore, the highly sensitive respond to pH being helpful to determine the target is one important point to make ZIF to be a promising drug delivery and drug release.

Nano-particle ZIF-90 was engineered to be magnetic and was chosen to be a drug carrier in [25]. Small  $\text{Fe}_3\text{O}_4$  and  $\text{Gd}_2\text{O}_3$  nanoparticles were embedded into the core of ZIF-90 helping to increase the precise delivering of the drug. In [26], various methods were conducted successfully to synthesize ZIF-90 nano-particles which could be applied in drug delivery.

### 1.3.3. Sensor

ZIFs also exhibit the potential in sensor application, ZIF-90, for instance, they showed the ability to be a luminescent sensor due to the high selectivity capacity for metal ions, anions and organic molecules like  $\text{Cd}^{2+}$ ,  $\text{Cu}^{2+}$ ,  $\text{CrO}_4^{2-}$  and acetone [27].

### 1.3.4. Gas storage

With a very high pore volume and large surface area, gas storage is one of the most popular use of ZIFs in general. The post synthesis modification was used to increase the capture capability of  $\text{CO}_2$  in ZIF-90, such as the combination between ZIF-90 and ethylenediamine to change the aldehyde group to imine group or the hybrid ZIF-8-90 with the ratio 1:1 of organic ligand [28].

### 1.3.5. Gas and biofuel separation

As mentioned before, a moderate window size ( $3.5 \text{ \AA}$ ) and a remarkable stability in ZIF-90 are unique factors supporting the selectivity of gas mixtures or biofuel mixtures.

Huang et al. did the modification of the functional group from aldehyde to imine group in the organic ligand that could improve the separation factor of CO<sub>2</sub>/CH<sub>4</sub>, CO<sub>2</sub>/N<sub>2</sub> and hydrogen purification [7, 29]. Other groups showed the adsorption of methanol, ethanol, propanol or 1-butanol from water vapor in ZIF-90 which is useful for biofuel recovery.

Furthermore, mix-matrix membrane and hybrid ZIFs are emerging as new effective methods that increase the membrane separation factor in ZIF-90 or in the ZIFs family in general.

#### 1.4. Literature review

Based on a lot of interesting features, from 2008 until now, there are approximately fifty publications for studying ZIF-90 and one third of them are computational work or combined simulation and experiment. Many researchers do simulation to predict the properties of physical processes and finally a good agreement between computational results and experimental results has been found. Adsorption, diffusion, permeability, separation are the main problem that scientists are going on that. While the experimental researchers find the way to optimize or improve the capacity of materials by the synthesis, change method, the computational researchers try to find the most accurate models to understand and forecast features by simulation.

In 2010, Caro and his group used ZIF-90 as a membrane for hydrogen purification [8]. A novel strategy for ZIF membranes was produced based on the idea from previous work [3], Yaghi and co-operator synthesized not only ZIF-90 but also ZIF-92 through the imine condensation reaction. In this work, to enhance the performance for gas separation, APTES was used (3-aminopropyl tri-ethoxysilane) to be a linker between Al<sub>2</sub>O<sub>3</sub> support with ZIF-90 via that reaction. In the following research, they tried to develop their method which can contract the window diameter and decrease the inter-crystalline defects. The obtained results show a remarkable high

separation factor which is a proof for the high potential of this material for gas separation [7-9, 29].

In 2011, in a simulation work, Amrouche et al [30] studied the role of functional groups in CO<sub>2</sub>, CO, CH<sub>4</sub> and N<sub>2</sub> adsorption, therefore, they examined ZIF-8 (-CH<sub>3</sub>) and varied from the original methyl group to others ( -CHO, -COOH, -NO<sub>2</sub>, -Cl). Because ZIF-NO<sub>2</sub> and ZIF-COOH have not been synthesized, DFT-calculation was applied to optimize all of them for a good consistency and MC simulation with Grand Canonical (GC) ensemble for the adsorption. From the obtained results, they proposed that the electrostatic interaction will play a crucial part in CO<sub>2</sub> or other gas molecules which have a high dipole or quadrupole moment and therefore, have stronger electrostatic interaction. Based on that, they suggest the functionalization for improving the separation. However, they stop to concern about the adsorption and did not mention about the diffusion that is also important for the gas separation process.

In 2012, Thornton et al [11] did both MD and MC simulation to predict and explore the high potential of all ZIFs in gas selectivity. They obtained self-diffusion coefficients by MD, conducted MC simulation for getting adsorption and then predict the permeance through these results. However, they did not include the charge for their model during calculation. Furthermore, they concerned mainly on ZIF-11 so they tried to modify DREIDING force field to fit with the experimental data. Therefore, this might affect the results for other ZIFs such as ZIF-90.

In 2012, Atci and Keskin investigate the performance of adsorbing and diffusing single gas or mixture gas in 15 different ZIFs, some of whom come from their previous work [10]. The UFF force field again was used in this work for simulation and compared with the DREIDING force field. Like above mentioned work, they also investigated their models with Grand canonical Monte Carlo (GCMC) and equilibrium molecular dynamics (EMD) simulations and predict the adsorption-based, permeation-based, permeability. Furthermore, a good agreement is obtained between performing simulation and calculating by mixing theories for estimate diffusion-based selectivity. Nevertheless, when comparing with experiment, they found the underestimate of CH<sub>4</sub> and N<sub>2</sub>

permeance in mixture and therefore it will lead to overestimate the selectivity in mixture gas. The main reason came from their assumption of rigid frameworks for saving the computational cost and examining a lot of ZIFs. Hence, gas molecules that have larger diameters than pore size of ZIFs would not pass or permeate through the membrane but of course, in reality, frameworks are flexible.

In 2012, an experimental work was also published in the same journal, Nair's group described properties of adsorption of  $\text{CH}_4$ ,  $\text{CO}_2$ ,  $\text{N}_2$  in two MOFs, one of them is ZIF-90 [31]. The experiment was carried out within a range of temperature from 30 to 70°C and pressure from 0.3 to 110 psi. Both of these MOFs have the same trend for gas solubility which is  $\text{CO}_2 > \text{CH}_4 > \text{N}_2$ . However, while MOF (Cu-hfipbb) showed a good agreement with mono-layer coverage in the Langmuir model, ZIF-90 only followed this rule at low pressure due to their capacity for multi-layer at high and moderate pressure which can be explained by the large pore volume inside and small window size (three dimensions).

In 2013, the first study about flexible lattice for ZIF-90 was published by Gee and co-worker [5]. Both approaches experiment and computation were used to study gas activities which are diffusion and adsorption inside ZIF-8 and ZIF-90. The structure of materials was taken from XRD data and then they tried to use their own force field which was optimized again by DFT-calculation, in their work, two force fields conducted were GAFF and DREIDING. For a flexible model, they use hybrid GCMC which can allow for the flexibility of aldehyde group. The results from adsorption simulations show a slight difference between rigid and flexible framework and ZIF-90 exhibits a higher potential for adsorbing alcohol based on their hydrogen bond. NVT MD simulation was applied to obtain the diffusion coefficient, the best agreement was obtained when using a flexible model with the GAFF force field comparing with PFG-NMR measurements. Although the gap between simulated and experimental value was quite big, they showed the same trend and so they can be used to predict the performance.

In 2014, Zhang et al [21] have examined a series of ZIFs to study the important role of the functional group in bio-fuel purification. Ethanol, water and the mixture between them were simulated with the UFF force field. Because of the results from above mentioned work which states that flexibility has not affected significantly the adsorption so in this work, they assume that framework to be rigid. Using molecular simulation results, they proposed ZIF-8 might be a good candidate for bio-fuel purification while ZIF-90 in this work show a good capacity for adsorb both ethanol and water because of hydrophilic functional group.

Recently, in both simulation and experiment areas, ZIF-90 has been mixed with another polymer to enhance the selectivity and the results show a remarkable separation factor [32, 33]. Therefore, understanding the potential of ZIF-90 is necessary and finding good force field parameters will help to obtain more reliable results. We simulate the different equilibrium states of guest molecules in ZIF-90 and investigate the adsorption, diffusion mechanisms comparing rigid and flexible frameworks. Many force fields of guest molecules will be checked and the results will be compared with experimental results to find the best force field parameters. The results attained, hopefully, can give more understanding of details in molecular scales and can be applied to the reality.

### 1.5. Scope of research

Various force fields of flexible lattice ZIF-90 and guest molecules will be tested employing rigid and flexible frameworks to obtain the best results for physical and chemical processes. Based on comparison with experimental data or theories, a better understanding and knowledge about the system (diffusion, adsorption, guest molecules behavior) can be attained.

The simulations will be carried out by MD (Molecular Dynamics) simulations at 300 K and 1 bar and GEMC (Gibbs Ensemble Monte Carlo) simulations to obtain the adsorption isotherm at 303 K in the pressure range from 0 to 255 bar. Hence, guest

molecules will be considered in the range of low, moderate and high concentrations inside the simulation box.



## CHAPTER 2

### THEORY BACKGROUND

#### 2.1. Simulation techniques

##### 2.1.1. Force field parameters

Force field refers the functional form or the set of parameter that describes the interaction of the atoms through calculating potential energy and forces of a given system. The general functional form of the potential includes two terms which are intra-molecular (bonded) and inter-molecular (non-bonded) potentials.

$$U_{total} = \sum U_{bonded} + \sum U_{non-bonded} \quad (2.1)$$

In which, each term can be clarified by

$$U_{bonded} = U_{bond} + U_{angle} + U_{dihedral} \quad (2.2)$$

$$\text{and } U_{non-bonded} = U_{van\ der\ Waals} + U_{electrostatic} \quad (2.3)$$

2.1.1.1. Bonded potential: consists of two-, three- and four-body interactions.

In equation 2.3, the bonded potential consists of two-, three and four body potentials as showed in Figure 2.1.

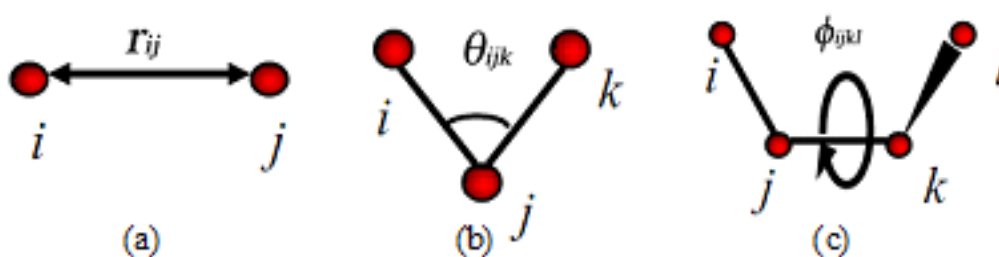


Figure 2.1. The bonded potential; a) bond stretching potential, b) angle bending potential, c) torsion angle potential [34].

Two-body bond stretching potential represents the harmonic vibration between atom  $i$  and  $j$  of a covalent bond (Figure 2.1a)

$$U_{bond} = \sum k_{bond}(r_{ij} - r_o)^2 \quad (2.4)$$

$k_{bond}$ : force constant, strength of the bond



$$r_{ij} = \|\vec{r}_j - \vec{r}_i\| : \text{distance between the atoms.}$$

$r_o$ : equilibrium distance

Three-body angle bending potential illustrates the harmonic potential for bending an angle, for example, angle is formed by three atoms (i-j-k)

$$U_{angle} = \sum k_{angle}(\theta_{ijk} - \theta_o)^2 \quad (2.5)$$

$k_{angle}$ : angle constant

$\theta_o$ : equilibrium angle

$\theta_{ijk}$ : angle ijk

$k_{angle}$  and  $\theta_o$  depend on the chemical types of atoms.

Four-body torsion angle potential describe the rotation around a bond between the planes formed by the first three and last three atoms of a consecutively bonded (i, j, k, l)-quadruple of atoms

$$U_{torsion} = \sum k_{torsion}[1 + \cos(m\phi_{ijkl} - \phi_o)] \quad (2.6)$$

$k_{torsion}$ : torsion angle constant

$\phi_o$ : equilibrium angle

$\phi_{ijkl}$ : angle ijk

$m$  is the *multiplicity*, which indicates the number of minima as the bond is rotated through  $360^\circ$

#### 2.1.1.2. Non-bonded potential

$$U_{non-bonded} = U_{van\ der\ Waals} + U_{electrostatic} \quad (2.7)$$

- Van der Waals potential: is the sum of repulsive and attractive force as described in Figure 2.2. The Lennard-Jones function is used most commonly to present the van der Waals potential function, see the equation 2.8.

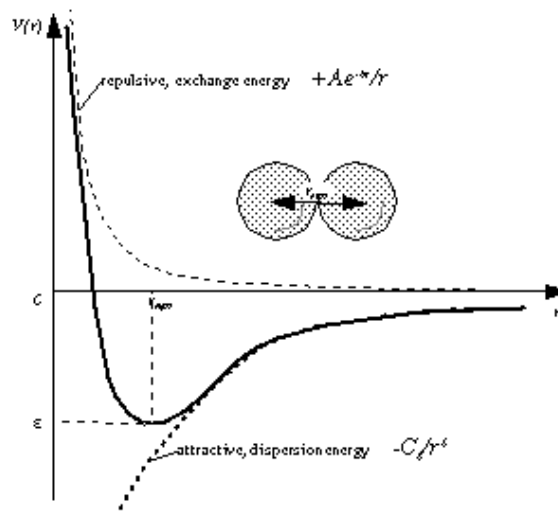


Figure 2.2. The van der Waals potential between two particles.

$$U_{van\ der\ Waals\ rij} = \sum_{i < j} 4\epsilon_{ij} \left[ \left( \frac{\sigma_{ij}}{r_{ij}} \right)^{12} - \left( \frac{\sigma_{ij}}{r_{ij}} \right)^6 \right] \quad (2.8)$$

In which,  $\epsilon_{ij}$  is the potential well-depth,  $\sigma_{ij}$  defines the distance between two particles  $i$  and  $j$ , where the LJ potential is zero. Finally, the potential reaches the minimum point at the distance  $r_{ij} = 2^{1/6}\sigma_{ij}$ .

Among many ways to calculate the parameters of hetero-nuclear molecules or mixtures, in this study, Lorentz-Berthelot combining rules are applied.

$$\sigma_{ij} = \frac{1}{2}(\sigma_{ii} + \sigma_{jj}) \quad \epsilon_{ij} = \sqrt{\epsilon_{ii}\epsilon_{jj}} \quad (2.9)$$

- Electrostatic potential: The electrostatic potential of a pair of atoms which have point charges  $q_i$ ,  $q_j$  are represented by Coulomb potential equation as showed in equation 2.10.

$$U_{Coulomb} = \sum_{i < j} \frac{1}{4\pi\epsilon_0} \frac{q_i q_j}{r_{ij}} \quad (2.10)$$

$\epsilon_0$  is the effective dielectric function for the medium,  $r_{ij}$  is the distance between two studied atoms  $i$  and  $j$ .

### 2.1.2. Periodic boundary conditions

In a small system, the percentage of particles locating at the surface is higher so that the surface effects will dominate. Therefore, unless surface effects are the

particular interest, periodic boundary conditions are usually applied. Figure 2.3 illustrate for the 2D example, one box is surrounded by other 8 boxes.

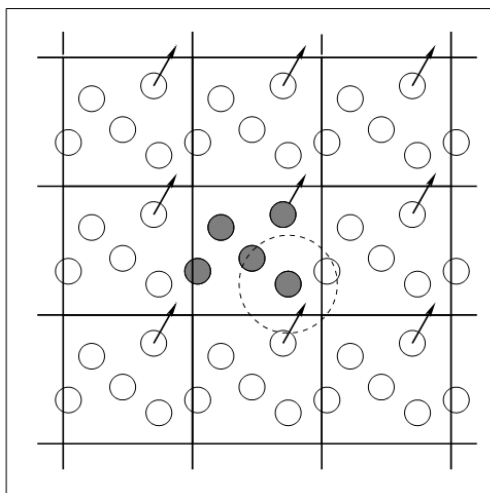


Figure 2.3. Periodic boundary condition [35].

The coordinates of the particles in the image boxes can be calculated by adding or subtracting multiples of the box length. During simulation time, whether particles move out of the simulation box, according to periodic boundary conditions, the image particles will enter from the opposite side simultaneously. Hence, the number of particles could be remained in the simulation box, they will interact not only with other particles in the central box but also with-images in the next boxes. The results obtained should be independent upon the choice of the initial position of the original box. The minimum image convention is applied to avoid the interaction between particles with their own images. In which, the forces on molecule  $i$  from molecule  $j$  are calculated only for the nearest one of all images of a particle  $j$ , no matter, if this particle is inside or outside the MD box [35].

The most common shape of the simulation box is the cubic box, however, there are still other shapes used to reduce the simulation time as much as possible depending on specific cases such as truncated octahedral or rhombic dodecahedral cells, *etc.*

### 2.1.3. Ensembles

The term “ensemble” is an artificial construct used to define as a collection of identical units or replicas of a system [36]. The different ensembles representing the same state of the system should produce consistent averages. However, some fluctuations still remain in various ensembles. Due to four main observable thermodynamic variables (or state variables) in a thermodynamic state which are number of molecules (N), pressure (P), temperature (T) and volume (V), Gibbs [37] defined three crucial ensembles according to the constant variables in each system

- Microcanonical ensemble (NVE ensemble): a statistical ensemble in which the number of particles in the system (N), volume (V) and the total energy (E) are fixed. This represents for an isolated system.

- Canonical ensemble (NVT ensemble): a statistical ensemble in which the number of particles (N), volume (V) and the temperature (T) of the system will be constant. The canonical ensemble is relevant for featuring a closed system being in weak thermal contact with a heat bath. The energy is allowed to exchange and the states of the system will be different in term of total energy.

- Grand canonical ensemble ( $\mu VT$  ensemble): a statistical ensemble describing an open system in which the energy and the particle number can be changed. Instead, both the temperature and chemical potential have to be specified.

In addition, the isobaric-isothermal ensemble (NPT ensemble) is characterized by the particle number (N), pressure (P) and temperature (T). The energy and the volume of the system can be exchanged through the heat bath and pressure bath, respectively.

### 2.1.4. Radial distribution functions (RDFs)

The Radial distribution function (RDF),  $g(r)$  is one kind of pair correlation function which describes how the density of particles varies as a function of distance from a given reference particle. In a simpler way, RDF gives the information about the

probability to find a particle at a distance  $r$  from the reference particle. In general, it is calculated by measuring the number of particles between the distance  $r$  and  $r + dr$  away from a given particles [34].

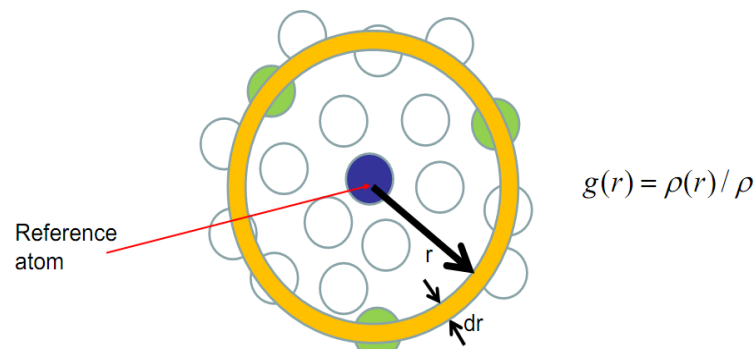


Figure 2.4. The radial distribution function (RDF) [34].

Specifically,  $g(r)$  is determined through the following equation

$$g_{ij}(r) = \frac{N_{ij}(r, r+\Delta r)V}{4\pi r^2 \Delta r N_i N_j} \quad (2.11)$$

Where  $g_{ij}(r)$  is the radial distribution function for sort  $i$  with sort  $j$ ,  $r$  is the distance,  $N_{ij}$  is the number of atoms of sort  $j$  around a given atom of sort  $i$  within the interval from  $r$  to  $r + \Delta r$ .  $V$  is the volume,  $N_i$  and  $N_j$  are the number of atoms of sort  $i$  and  $j$  in the MD box respectively.

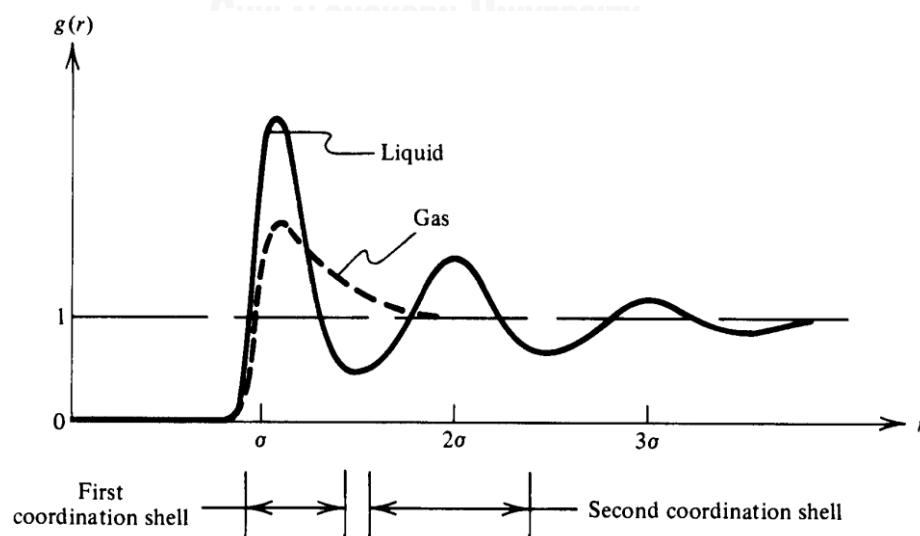


Figure 2.5. The radial distribution function for a simple fluid [34].

## 2.2. Gibbs Ensemble Monte Carlo simulation (GEMC)

The Gibbs ensemble Monte Carlo (GEMC) simulation is a useful technique for studying phase coexistence properties of e.g. fluid mixtures or, in our case of a gas phase and an adsorbed phase. It was first propounded by Panagiotopoulos in 1987. In GEMC, a two phase system without any interface is created, in which the temperature, pressure and chemical potential in these two phases need to be equal in equilibrium. In GEMC, the chemical potential does not appear explicitly, different from GCMC. In GEMC, particles can be exchanged between the different phases but, the total number of particles is fixed.

To perform GEMC, two simulation boxes which represent two phases being in equilibrium are set up. These phases are connected to a heat bath to maintain constant temperature of the system without interface between the two phases. The periodic boundary conditions are applied in the simulation. There are three types of the movements to achieve phase equilibrium which are displacements, rotation, and particles transfers in this work as shown in Figure 2.6 [38].

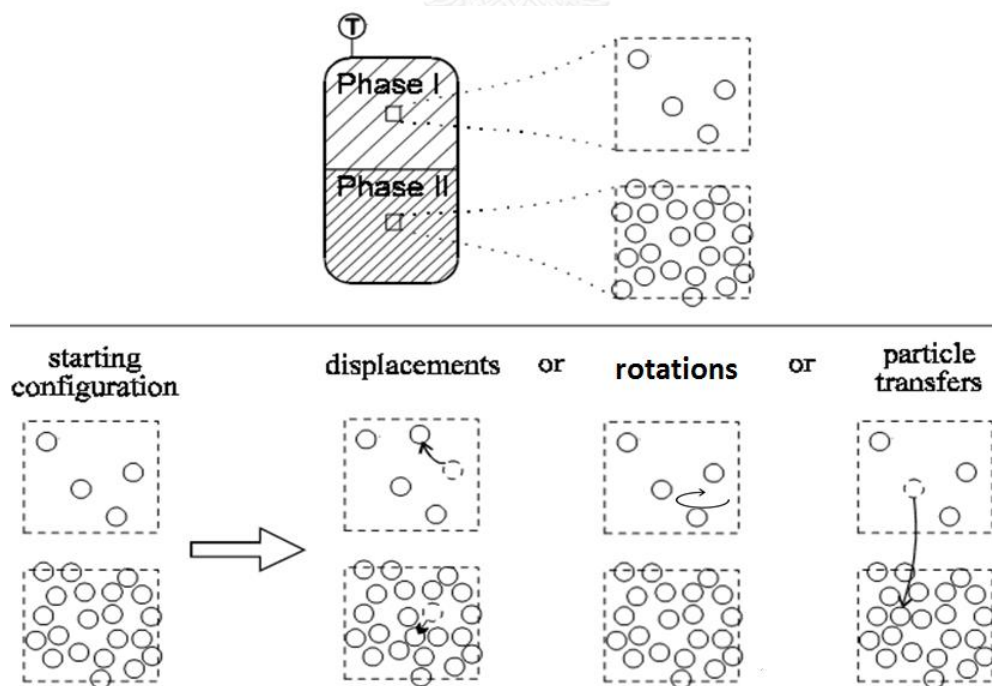


Figure 2.6. The possible movement in Gibbs Ensemble Monte Carlo [39].

- Particle displacement: A particle is allowed to move or rotate to some new positions randomly in the simulation box. In this case, a box is likely a system at NVT ensemble which fixes number of particles, volume and temperature, and the choice of the movement is following the normal Metropolis Monte Carlo algorithm.

- Particle transfer: one particle from one phase is removed and then inserted in another phase at a random position and in general random orientation except for spherical particles. This will allow the system exchange mass or the particle number with the condition of the equality of the chemical potential between the two phases which is guaranteed by the exchange acceptance criterion without explicit appearance of the chemical potential. During this perturbation, the coexisting phases are similar with the grand canonical ensemble ( $\mu VT$ ) in which each box has the same temperature and equal chemical potential.

### 2.3. Molecular dynamics simulation (MD simulation)

In general, molecular dynamics simulation (MD simulation) is performed by following the Newton's second law of motion in classical mechanics which is  $F = ma$ . Thus, MD is a type of N-body simulation. The advantage of MD simulation over MC is that MD helps to observe the dynamical properties like time dependent movement, diffusion or some spectra. MD does also yield all structural properties but, for structural properties MC is much more effective.

#### 2.3.1. Classical mechanics

Classical mechanics is the study about the motion of particles by applying the general principles of Newton's law of motion. In classical mechanics, the atoms are points that interact by interaction potentials and they can be connected by bonds etc. to form molecules.

Each point particle is characterized by a set of interaction parameters, like mass and Lennard-Jones parameters. Its state is described by position and velocity. In MD

simulation, the trajectory is found by the solution of the classical equations of motion which is written

$$\vec{F}_i = m_i \vec{a}_i \quad (2.12)$$

where  $\vec{F}_i$  is the total forces of atom  $i$ ,  $m_i$  is the mass and  $\vec{a}_i$  is the acceleration of atom  $i$ .

Therefore, in order to get the updated positions of particles, the forces have to be calculated and these are the first derivatives of the potential energy ( $U$ ). The potential energy is calculated from the interaction force fields that is mentioned above. So that the relationship between the potential energy with the changing of the position as a function of time ( $t$ ) can be shown in equation 2.15.

$$\vec{F}_i = -\frac{\partial U}{\partial \vec{r}_i} = m_i \frac{\partial^2 \vec{r}_i}{\partial t^2} = m_i \vec{a}_i \quad (2.13)$$

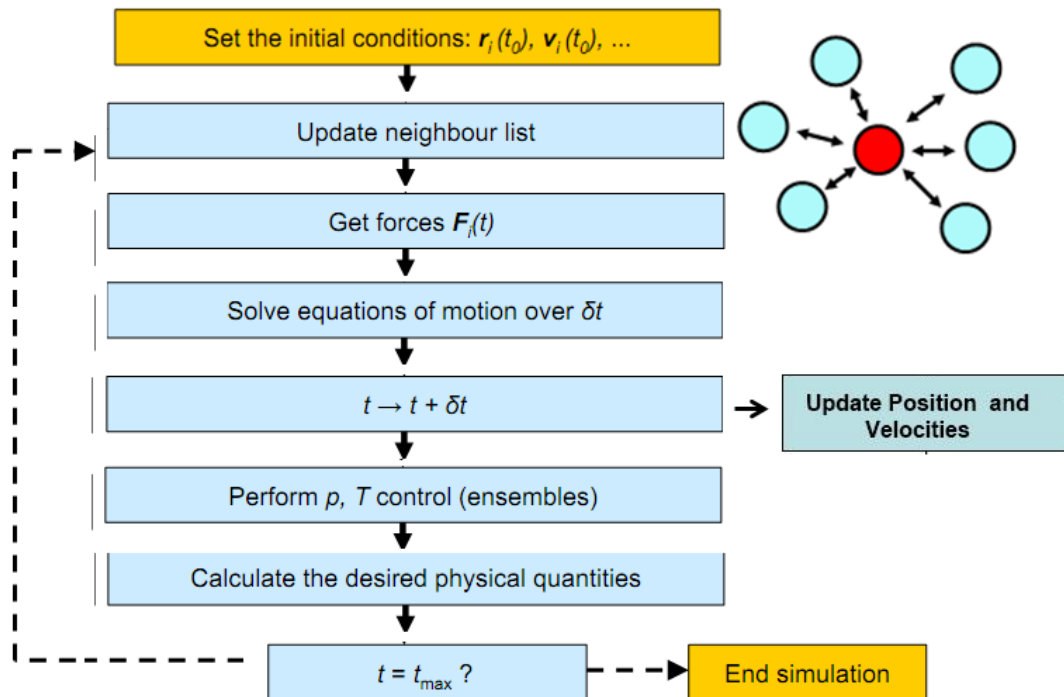
The initial positions and velocities of the guest molecules in the system are normally created randomly while the positions of the lattice atoms follow from the experimental crystal structure. The later positions and velocities follow from the solution of the equation of motion. In addition, based on Maxwell-Boltzmann or Gaussian distribution at a specific temperature, the initial velocities are chosen to fulfill

$$\vec{P} = \sum_{i=1}^N m_i \vec{v}_{i0} = 0 \quad (2.14)$$

The trajectories will provide all the positions and velocities of all particles in the system during the simulation time, from them the dynamical properties can be obtained.



MD simulation is conducted as the following diagram [39]



- Set the initial conditions for the simulation in terms of the initial coordinates and initial velocities of the particles in the system.
- The list of neighbor will be updated after every time step.
- Solve the equations of motion to find the new positions and velocities.
- Update new configuration and velocities
- Perform pressure or temperature control depending on different ensembles
- Repeat these processes until the time reach the time simulation that is set up at the beginning.
- From the trajectory, analyze the result to get many physical quantities and dynamical properties of the system.

### 2.3.2. Algorithm

In MD simulation, if the initial coordinates and velocities are known, then the coordinates and the velocities at any time can be found by the Newton equation of motion

$$\vec{F}(t) = m \frac{d\vec{v}(t)}{dt} \quad (2.15)$$

To solve this differential equation, many different methods are used such as the Leapfrog, the Verlet, the Toxvaerd and the Gear algorithms. However, these algorithms need to satisfy some following criteria to be a good algorithm

- being fast and costing little computer memory
- allowing the use of a relatively long time step
- performing a good energy and momentum conservation.

The Verlet algorithm being one of the most common ways in MD simulation is applied in this work. In Verlet algorithm, the central difference is used for the approximation of the slope

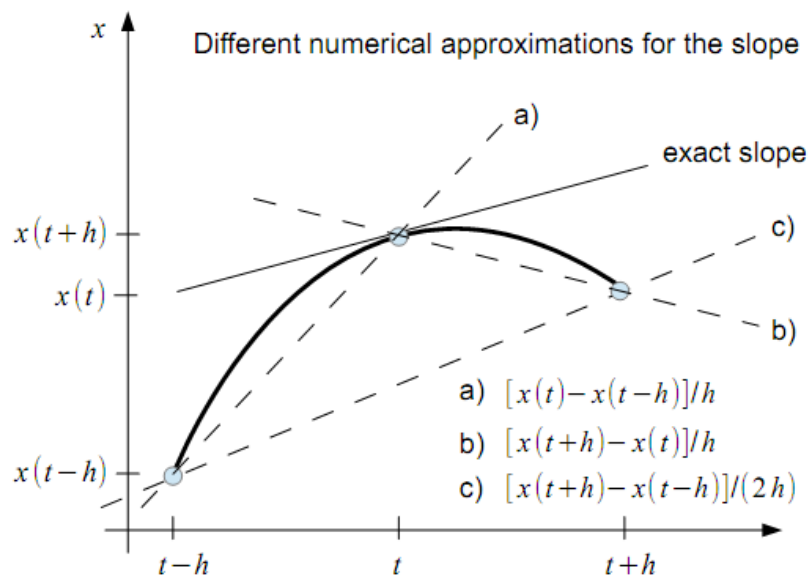


Figure 2.7. The different numerical approximations for the slope [40].

Using Taylor expansion to determine the position from time  $t$  to time  $t+h$  along the trajectory

$$\vec{r}_i(t+h) = \vec{r}_i(t) + \vec{v}_i h + \frac{h^2}{2} \ddot{\vec{r}}_i(t) + \frac{h^3}{6} \dddot{\vec{r}}_i(t) + \dots \quad (2.16)$$

For the time  $-h$

$$\vec{r}_i(t-h) = \vec{r}_i(t) - \vec{v}_i h + \frac{h^2}{2} \ddot{\vec{r}}_i(t) - \frac{h^3}{6} \dddot{\vec{r}}_i(t) \pm \dots \quad (2.17)$$

Then the sum of both gives

$$\vec{r}_i(t+h) = 2\vec{r}_i(t) - \vec{r}_i(t-h) + h^2 \ddot{\vec{r}}_i(t) + O(h^4) \quad (2.18)$$

Thus, the equation of the Verlet algorithm up to 4<sup>th</sup> order in the Taylor expansion is

$$\vec{r}_i(t+h) = 2\vec{r}_i(t) - \vec{r}_i(t-h) + h^2 \ddot{\vec{r}}_i(t) \quad (2.19)$$

On the other hand, the velocities needed to calculate the kinetic energy can be obtained from the central difference

$$\vec{v}_i(t) = [\vec{r}_i(t+h) - \vec{r}_i(t-h)]/(2h) \quad (2.20)$$

This algorithm is simple but has a very good numerical stability for the large time step and other necessary physical properties like time reversibility or cheap computer cost, *etc.*

## 2.4. Gas transport

### 2.4.1. Mechanism of gas transport

There are difference mechanisms for transport of gas molecules through a porous membrane [41].

- Knudsen diffusion: applied for the membrane which have a small pore diameter while the mean free path for gases is much larger, so gas molecules will dominantly interact with the pore membrane more than with each other. The Knudsen selectivity of gas mixture 1:1 can be calculated by square root the proportion of molecular weight two gases.

$$\alpha_{K,A/B} = \sqrt{\frac{M_{WB}}{M_{WA}}} \quad (2.21)$$

- Molecular sieving: gases can be separated from this membrane based on the difference kinetic diameter. Gases, which have smaller diameters than pore diameters

of the membrane, will be allowed to pass through membranes. Therefore, molecular sieving membranes selected must have pore diameter between kinetic diameters of gas molecules that need to be separated. The selectivity in this type is very high.

- Solution-diffusion: In this case, the solubility of gases in membrane is different and the diffusion through membrane also depends on intrinsic properties of gases and membrane. Hence, the permeance of gases is different leading to gas separation (in polymer, metal)

- Adsorption-diffusion (surface diffusion): This process occurs in three steps, the adsorption in the membrane, the diffusion through membrane and the desorption from one adsorption site to another site. Zeolites, mesoporous carbon and MOFs are in use to employ this mechanism.

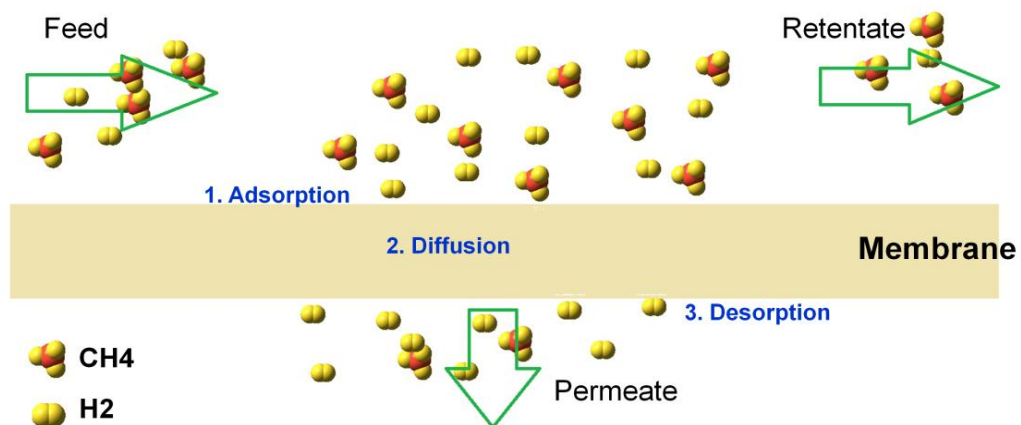


Figure 2.8. The mechanism of CH<sub>4</sub>/H<sub>2</sub> transport through a membrane with surface diffusion

#### 2.4.2. Diffusion, Adsorption and Permeability

To understand more about the activities of gas molecules in ZIFs, the diffusion, adsorption and permeability will be considered in this section

- Adsorption: gas molecules-adsorbate will be accumulated on the surface of ZIFs-adsorbent. There are mainly two forces for this process which are (i) electrostatic force and (ii) van der Waals force. ZIFs having polarized functional group such as ZIF-

90 (CHO), ZIF-NO<sub>2</sub>, ZIF-COOH will interact better with gas molecules which have high dipole moment or quadrupole moment (CO, CO<sub>2</sub>) than others (CH<sub>4</sub>, N<sub>2</sub>). In mixture gases *i* and *j*, adsorption selectivity can be evaluated by this equation

$$S_{adsorption(i/j)} = \frac{x_i/x_j}{y_i/y_j} \quad (2.22)$$

*x* is the molar fraction of the adsorbed phase

*y* is the molar fraction of the bulk gas phase

From this equation, one can predict the adsorption selectivity based on the simulation result from MC simulation and also from the experiments or MD simulations

- Diffusion: it is the natural transport of molecules (or ions, atoms) from a high concentration region to lower concentration region by their random thermal motion in contrary to streaming which is a collective motion following the pressure gradient. Diffusion in porous materials or in ZIFs was reviewed in detail by Gavalas et al [42] and Krishna et al [43]. In which, two kinds of diffusion that can be calculated or measured are transport diffusivities and self-diffusivities. While transport diffusivity is determined by Fick's law [44] and measured under non-equilibrium condition, self-diffusivities are measured under equilibrium condition which are define by IUPAC are the diffusion coefficient when the chemical potential gradient is equal to zero. It shows somehow the mobility of guest molecules inside the framework without any gradient.

In more detail, to calculate the self-diffusion coefficient (*D<sub>s</sub>*), there are two main ways to get it, (i) Green-Kubo relation and (ii) Einstein relation.

(i) Self-diffusivities are calculated from velocity autocorrelation function

$$D_s = \frac{1}{3} \int_0^{\infty} \langle v_i(0) \cdot v_i(t) \rangle dt \quad (2.23)$$

(ii) The relation between self-diffusivities and the mean square displacement

$$D_s = (1/6t) \langle \{r_1(t) - r_1(0)\}^2 \rangle \quad (2.24)$$

In mixture, diffusion selectivity can be evaluated like that, in which self-diffusivities measured in mixture

$$S_{diffusion(i/j)} = \frac{D_{s,i(i,j)}}{D_{s,j(i,j)}} \quad (2.25)$$

- Permeability: to calculate permeability, we need permeance which is flux within the membrane ( $N_i$ ) divided by the log difference of partial pressure between the retentate and permeate ( $\Delta P_i$ )

$$\Pi_i(\text{mol.m}^{-2}.\text{s}^{-1}.\text{Pa}^{-1}) = \frac{N_i}{\Delta P_i} \quad (2.26)$$

Then permeability will be

$$P_i(\text{mol.m}^{-1}.\text{s}^{-1}.\text{Pa}^{-1}) = \Pi_i l \quad (2.27)$$

$l$  is top-layer thickness

In porous material, due to the porous structure, the gas transport mechanism inside follows the surface diffusion. Hence, the permeance can be predicted by the combination of the adsorption and the self-diffusion coefficient as the following equation

$$P_i = \Pi_i l = D_{s,i} \phi \frac{c}{f} \quad (2.28)$$

$\phi$  is void fraction,  $c$  ( $\text{mol.m}^{-3}$ ) is equilibrium gas concentration,  $f$  (Pa) is the fugacity.

Furthermore, permeation selectivity can also be evaluated by the relation

$$\begin{aligned} S_{\text{permeation}} &= S_{\text{adsorption}(i/j)} \cdot S_{\text{diffusion}(i/j)} \\ &= \frac{x_i/x_j}{y_i/y_j} \cdot \frac{D_{s,i}(x_i,x_j)}{D_{s,j}(x_i,x_j)} \end{aligned} \quad (2.29)$$

$S_{\text{adsorption}(i/j)}$ ,  $S_{\text{diffusion}(i/j)}$  are adsorption selectivity and self-diffusion selectivity respectively

## CHAPTER III

### CALCULATION DETAILS

#### 3.1. Model and force field parameters

The structure of the ZIF-90 framework was obtained from the Cambridge Crystallographic Data Centre (CCDC), determined by Morris et al. [3]. The simulation box consists of  $2 \times 2 \times 2$  unit cells in the Molecular Dynamics (MD) simulation and  $4 \times 4 \times 4$  unit cells in the Gibbs Ensemble Monte Carlo (GEMC) simulation. The diffusion of methane molecules can only proceed through the 6-membered rings that connect adjacent cavities. They are called ‘window’ in the following. Other connections between the cavities are too small to allow the passage of methane molecules.

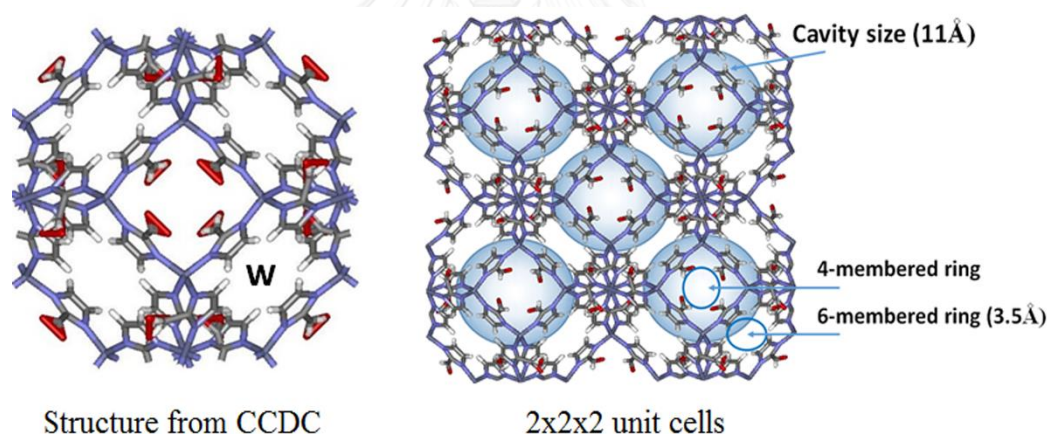


Figure 3.1. Structure of ZIF-90. The 6-membered ring is called ‘window’ (w in the left part of the picture).

From a literature review [5, 20, 45] we found that the most common force fields for the framework that could produce a stable lattice size and dynamical properties were that of GAFF (which is a generalized AMBER force field) [5] and that of DREIDING [5]. Therefore, GAFF and DREIDING as well as modifications of them were tested in this work to describe both the bonded interactions (bond, angle, torsion and dihedral) and the non-bonded interactions (van der Waals interactions).

The charges of atoms, collected in Table 3.1, were calculated by the DDEC method [5] and then slightly modified in order to neutralize the system as documented in Table 3.1.

Table 3.1. Partial charges of the atoms in the ZIF-90 framework (the name of atom type can be found at figure S1 in the appendix).

| Atom type           | Charge (Gee et al [5]) | Adjusted charge |
|---------------------|------------------------|-----------------|
| C_CR                | 0.2104                 | 0.21            |
| C_CC                | -0.0001                | -0.002          |
| C_CT                | 0.2582                 | 0.258           |
| H_H4                | 0.1149                 | 0.115           |
| H_HT                | 0.0476                 | 0.049           |
| Zn                  | 0.6726                 | 0.674           |
| O                   | -0.4091                | -0.41           |
| N                   | -0.332                 | -0.335          |
| total charge of the |                        |                 |
| lattice             | 1.728                  | 0               |

In addition, the five different tested force fields of CH<sub>4</sub> are shown in Table 3.2. CH<sub>4</sub> was treated as a spherical molecule in the force fields 1 (FF1) to 4 (FF4) and as a flexible molecule model containing 5-interaction centers in the force field 5 (FF5).



Table 3.2. Force fields for methane

| Source  | Molecules           | $\epsilon$ (K) | $\sigma$ (Å) | charge |
|---------|---------------------|----------------|--------------|--------|
| FF1[46] | CH <sub>4</sub>     | 158.5          | 3.72         | 0      |
| FF2[14] | CH <sub>4</sub>     | 147.9          | 3.73         | 0      |
| FF3[47] | CH <sub>4</sub>     | 173.2          | 3.8842       | 0      |
| FF4[48] | CH <sub>4</sub>     | 191.235        | 3.71         | 0      |
| FF5[49] | C(CH <sub>4</sub> ) | 30.7           | 3.74         | -0.24  |
|         | H(CH <sub>4</sub> ) | 14.1           | 2.67         | 0.06   |

### 3.2. Gibbs Ensemble Monte Carlo simulations (GEMC)

For the GEMC simulations, the in-house simulation software ‘Gibbon’ was used like done before in refs. [16, 18]. A combination of GEMC and MD by DL\_POLY was also applied in [18] where the different lattice structures for lower and higher pressures as obtained from flexible lattice MD were used for GEMC simulations. This was not done in [16, 18] because in the pressure range that was investigated by GEMC in these papers only one structure existed.

In GEMC two simulation boxes were set up, box A and box B. Box A contained guest molecules (CH<sub>4</sub>) in bulk free gas, and box B represented 4×4×4 unit cells of the ZIF-90 framework with adsorbed methane guest molecules. At low pressure of 0-1 bar, the system was run 10<sup>5</sup> steps until equilibrium could be stated by observing stable uptake in box B and agreement of the chemical potentials in both boxes. Then an evaluation part of 10<sup>6</sup> steps was started. At higher pressure (up to 255 bar), 10<sup>6</sup> steps were necessary to approach to equilibrium and the evaluation part was then 10<sup>7</sup> steps.

The temperature was chosen to be 303 K for a comparison with the experimental data of [31] for testing the force fields. But the temperature was set 300 K for studying other system properties corresponding to the results in MD simulations.

Using the Gibbon software for GEMC simulations, in each simulation step there is first a random decision if a trial of a shift or rotation of a randomly chosen molecule

in box A or box B takes place, or if a particle is tried to be swapped from one box to the other one. If a swap is to be tried then according to [50] first one of all particles is chosen randomly, no matter in which box it is, and then a trial to swap it is accepted or not with the proper probability given in [50]. This will lead to an equilibrium between the gas phase and the adsorbed molecules.

In Gibbon the Coulomb interactions are not calculated by the computer time expensive method of Ewald summation. First in [51] it has been shown that in many particle systems, which are neutral in sum of the charges, for large distances Coulomb interactions are reduced by many-particle effects and can be dropped down by shifted forces or similar models. This technique has meanwhile been used in many papers *e.g.* in [18, 52]. In the Gibbon software the Coulomb interactions are dropped down smoothly at a cutoff distance of 30 Å. The box size used in GEMC is 69.086 Å. Note however that the efficiency of the method is strongly improved by switching off all Coulomb interactions of a given, in sum neutral molecule with another charge (belonging to the ZIF lattice or to another guest molecule) at once. The reason is that the Coulomb interaction between two isolated partial charges can be several kJ/mol even at 30 Å. Besides, the sum of the interactions of the complete molecule with one other partial charge is normally orders of magnitude smaller at this distance, then only quadrupole moments and higher multipole moments need to be cut off. This balance of charges would be destroyed if the Coulomb fields were switched off atom by atom. The procedure is described in details in the appendix.

The cutoff for the vanderWaals forces (Lennard-Jones) has been chosen to be 14 Å like in the MD simulations.

While in Grand Canonical Monte Carlo (GCMC) simulations the loading of the ZIF with guest molecules is found as a function of the chemical potential, GEMC provides the exact information about which gas phase density outside of the ZIF corresponds to a given loading of the ZIF with guest molecules.

Hence, in the GEMC simulations the pressure can be evaluated in the gas phase while this would be ambiguous within the ZIF crystal. On the other hand, the chemical

potential for comparison is usually not available from adsorption experiments while the corresponding gas phase density is usually known.

The pressure in the gas phase can be calculated directly from the virial theorem or from an equation of state based on the density of particles. The Peng-Robinson equation of state [53] was chosen in this work to calculate the pressure. Thus, the amount of guest molecules adsorbed in ZIF-90 could be found as a function of the gas phase pressure.

During GEMC simulation, ZIF-90 was assumed to be rigid because previous papers about guest molecules adsorbed in ZIF's showed that the effect of the lattice flexibility on adsorption was not significant [16, 17]. In this work, GEMC served as a touch-stone for a reasonable force field for ZIF-90 and as a tool to examine static properties of the adsorbed guest molecules like radial density functions (RDF's) *etc.* It was interesting to compare RDF's from GEMC with rigid lattice with those of MD with flexible lattice in order to check the reliability of the rigid model for static properties.

### 3.3. Molecular Dynamics simulations (MD)

The force fields which gave good results for the adsorption isotherm were used to study also dynamical properties and the structure of ZIF-90 in MD simulations. From previous work [12-15], it is known that dynamical properties like the self-diffusion coefficient of guest molecules in many different ZIFs strongly depend on the flexibility of the framework. In this work, the MD simulation was conducted on both rigid and flexible frameworks to compare the results and find out the importance of the structure flexibility of ZIF-90 for methane as guest.

All MD simulations in this work were run by DL\_POLY 2.20 [54]. First the box length of the MD simulation box containing  $2 \times 2 \times 2$  unit cells ( $34.543 \text{ \AA}$ ) was checked in isothermal-isobaric (NPT) ensemble MD for the flexible framework as a first test of the interaction parameters. For this purpose the NPT simulations were carried out for 1 ns to relax the system to equilibrium and then additional 2 ns served to collect data

which were then compared with the experiment. The cutoff for van der Waals forces was 14 Å.

The dynamical properties were observed from micro-canonical ensemble Molecular Dynamics (NVE-MD). In these simulations the box size is constant per definition and has exactly the value given in the database from experiment. But, in the flexible lattice each of the 8 unit cells can still fluctuate in size and, more important for diffusion, also the size of the windows connecting adjacent cavities will fluctuate. The average value of the window size should agree with the value from the structure database.

First, to control the temperature of the system, isochoric-isothermal ensemble (NVT) MD simulation was conducted for 5 ns. After that, the system was allowed to equilibrate for 0.5 ns and then the dynamical properties were examined during 10 ns in the NVE ensemble.

The window size distribution and the self-diffusion coefficient can be evaluated from the trajectories of these runs. Loadings of 0.5, 2.5, 10 and 15 CH<sub>4</sub> molecules/cage inside ZIF-90 were examined. The temperature is fluctuating in NVE but the average was always closer than 1 per cent to 300 K in the MD runs.

The results were compared with available experiments and they were used to study—adsorption sites and self-diffusion coefficients as well as the membrane permeance.

## CHAPTER IV

### RESULTS AND DISCUSSION

#### 4.1. Methane in ZIF-90

##### 4.1.1 Test of different force fields for the simulation of adsorption isotherm and the structure of ZIF-90.

GAFF and DREIDING (DREID.) force fields for the framework and five different force fields of methane were applied to calculate adsorption isotherms at low pressure and 303 K by GEMC and to compare the results with experiments. The results are shown in Figure 4.1a. At these low pressures the ideal gas formula is used for the pressure calculations and thus the different molecular models do not have influence on the pressure calculations.

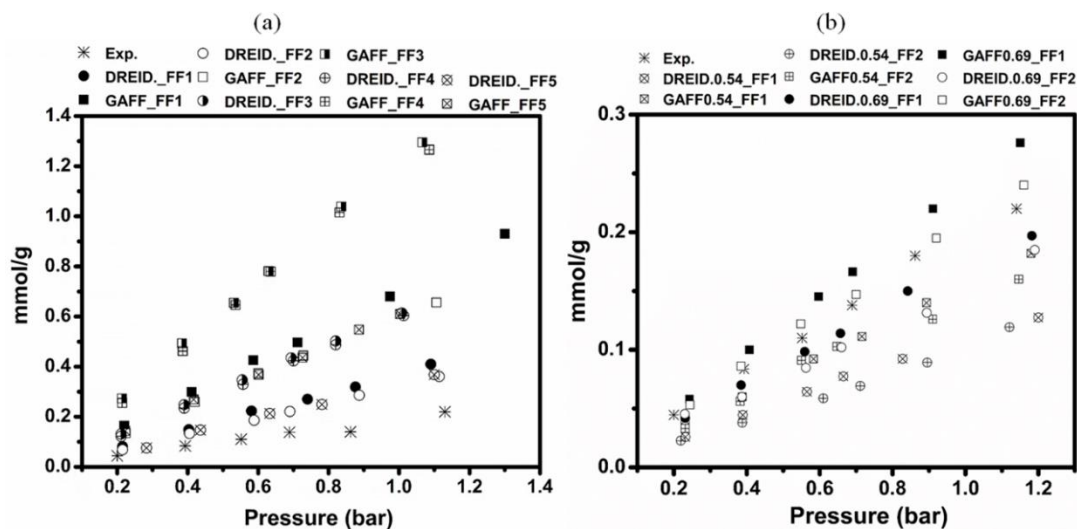


Figure 4.1. a) Comparison of adsorption isotherms of five force fields for  $\text{CH}_4$  (FF1-FF5) in ZIF-90 (GAFF and DREID.) at 303 K, b) the adsorption isotherm of  $\text{CH}_4$  in ZIF-90 at 303 K after scaling the force field of the framework. Experimental data from Venkatasubramanian et al.[31].

Note: The adsorption experiments [31] have been done at 303 K, therefore, we did GEMC simulations also at 303 K for comparison to test our parameters. These parameters have then been used for our MD simulations. In NVE – MD the temperature

as calculated from the kinetic energy fluctuates. In all runs the average temperature was within 1 per cent close to 300 K. We carried out additionally for different average temperatures within 1 per cent to 300 K. The results agreed within the range of fluctuations.

Figure 4.1a shows that there is no force field which can produce the adsorption isotherm well. This is clearly due to the fact that the contribution of the van der Waal attraction to adsorption is overestimated. This overestimation was also found in other previous works for water and alcohol adsorption in ZIF-90 [5, 10]. Hence, the well-depth was scaled by the scaling factor obtained from Pérez-Pellitero et al. [45]  $\epsilon^* = 0.69\epsilon$ ,  $\sigma^* = \sigma$  and Zhang et al [20]  $\epsilon^* = 0.54\epsilon$ ,  $\sigma^* = \sigma$  for both GAFF and DREIDING force fields. We call GAFF scaling 0.69 (GAFF 0.69), GAFF scaling 0.54 (GAFF 0.54), DREIDING scaling 0.69 (DREID. 0.69), DREIDING scaling 0.54 (DREID. 0.54) (see Table in the appendix). We performed that scaling with only two popular force fields of guest molecules (FF1 and FF2) because these two force fields of methane have shown a good performance in many previous publications. The adsorption isotherms obtained after modifying the force fields are shown in Figure 4.1b.

It can be seen from Figure 4.1b, that the modified GAFF (GAFF 0.69) and the modified DREIDING (DREID. 0.69) force fields can produce better results for adsorption isotherms when they were compared with the others. Therefore, GAFF 0.69 and DREID. 0.69 force fields were chosen to further study of the structure and dynamical properties. Moreover, the GAFF force field can produce the lattice constant better than the DREIDING force field mentioned in the previous work [5]. So that to compare the effect of the scaling factor on the structure of the ZIF and its dynamical properties, GAFF was studied in this work.

On the other hand, GEMC was also conducted to evaluate adsorption isotherms with the force field developed by Thornton et al. [11]. In their work, they modified DREIDING to get a good adsorption isotherm from Grand Canonical Monte Carlo ensemble (GCMC). In this work, we found by GEMC with modified DREIDING also good agreement with the experiment. These results also show good agreement between

the two methods GEMC and GCMC simulations for the adsorption isotherm as it has been expected.

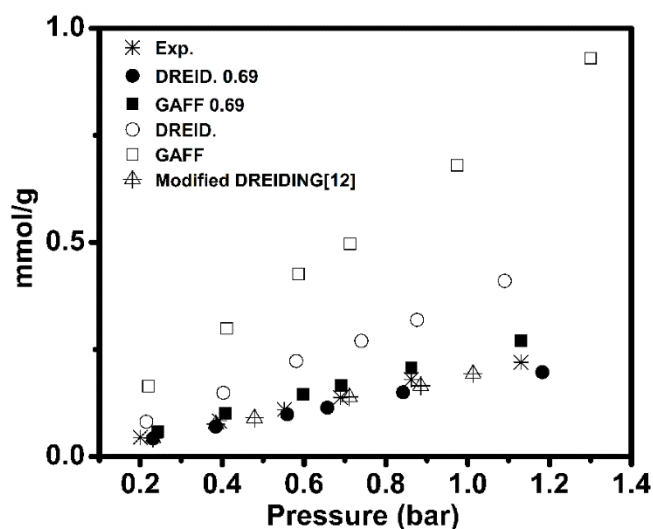


Figure 4.2. Adsorption isotherm of  $\text{CH}_4$  in ZIF-90 at 303 K for low pressure (0-1.2 bar) obtained from GEMC for the force field with and without modification. Experimental data from Venkatasubramanian et al. [31].

For examining the dynamical properties, in this work the NVE ensemble MD has been used because the calculation of the pressure (that is essential for NPT simulations) e.g. by the virial theorem for molecules in pores, particularly in the high pressure region is questionable. For example the cutoff correction to the virial result is well defined for gases and liquids but not for the molecules in pores. The importance of this correction increases in gases and liquids with the square of the density. Moreover, the scaling of intermolecular distances but, not of intramolecular distances, as usually done in NPT simulations, is questionable. In contrary, in NVE all quantities are well defined and the simulation box size corresponds to the structure of the database by definition. Nonetheless, the sizes of the different unit cells included in the MD box can still fluctuate. The most important structural feature for diffusion is the window size, controlling the migration of particles that must be reproduced well by the flexible lattice.

Nevertheless, as one property of the parameter sets, we additionally checked, which box size they would yield in NPT simulations, just as an additional information.

The distribution of the box length in NPT was shown in Figure S2 in the appendix and Table 4.1 gathering together the results from GAFF, GAFF 0.69 and DREID. 0.69 force field model and experiment. It can be seen from Table 4.1 that while GAFF and GAFF 0.69 force fields can hold a box length fitting with the XRD structure, the box length from DREID. 0.69 collapsed. The same results have been found in Gee et al. [5]. In addition, the window size was studied by analyzing results from NVE ensemble MD. From the distribution of window sizes in Figure 4.3 and data in Table 4.2, it was confirmed again that the better structures were gained from GAFF and GAFF 0.69 force fields. The window size in ZIF-90 from DREID. 0.69 (3.735 Å) is quite larger than GAFF (3.555 Å), GAFF 0.69 (3.525 Å) and experiment (3.5 Å). The smaller width of the window size distribution of modified DREIDING in comparison to GAFF and modified GAFF indicates a smaller flexibility as already found for ZIF-8 in [14]. In [14] this prevented the diffusion of methane even with flexible DREIDING but, in ZIF-90 the window size is somewhat larger than in ZIF-8.

From these above results, it is concluded that the modified GAFF can produce not only the adsorption isotherms that fit to the experiment but can also keep the structural quantities like box size in NPT and, more important, window size, well. On the other hand, modified DREIDING just only gives adsorption isotherms in good agreement with the experiment.

Table 4.1. The box length distribution that was obtained from NPT ensemble MD

|                | Exp. [3] | GAFF   | GAFF 0.69 | DREID. 0.69 |
|----------------|----------|--------|-----------|-------------|
| Box length (Å) | 34.543   | 33.440 | 33.540    | 32.565      |



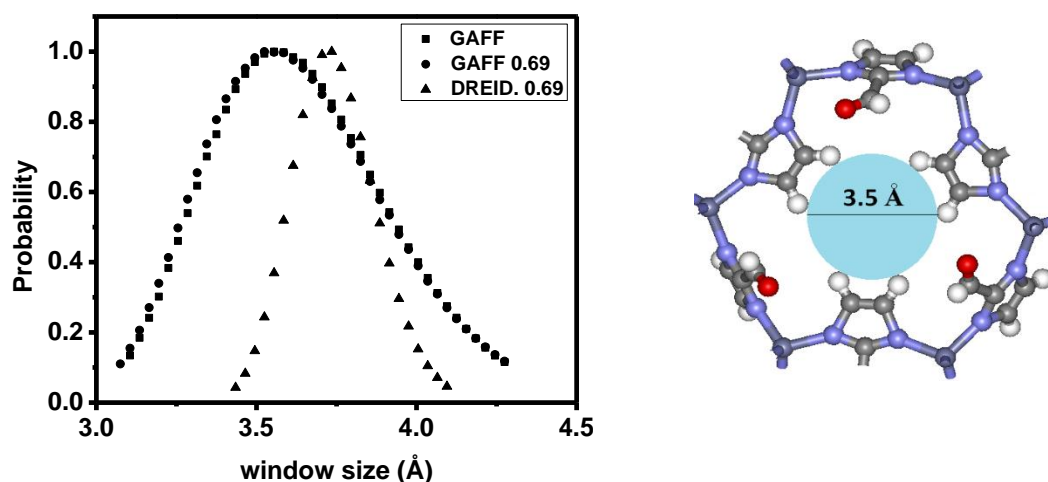


Figure 4.3. Distribution of the fluctuating window size of the flexible ZIF-90 framework without guest molecules at 300 K.

Table 4.2. Comparison of window sizes of ZIF-90 from different force fields with the experiment.

|                 | Exp.[3] | GAFF | GAFF 0.69 | DREID. 0.69 |
|-----------------|---------|------|-----------|-------------|
| Window size (Å) | 3.50    | 3.56 | 3.53      | 3.74        |

#### 4.1.2. Static properties

The static properties of guest molecules include radial distribution functions (RDF's) and probability density plots evaluated from the results in NVE ensemble MD with modified GAFF. Some RDF's are compared with those from GEMC.

Probability densities of methane in ZIF-90 during 5 ns simulation time in both rigid and flexible models are plotted in Figure 4.4. The red dots represent the sites of guest molecules (methane) in snapshots taken every 100 steps from the last 50000 steps to visualize the probability density to find methane at different sites of the framework. As we can see from Figure 4.4, the density clouds of methane molecules are connected with each other in a flexible framework while they are isolated in the rigid framework.

In the rigid model, methane molecules cannot pass through the narrow aperture to enter the next cage. Hence, they only move within the cage. The reason is that the diameter of methane (3.8 Å) is bigger than the window size in ZIF-90 (only 3.5 Å). However, due to the flexibility of the framework, methane molecules can pass the windows in moments in which the window size is temporarily larger than the average window size [55]. Interestingly, our MD simulation showed that in Figure 4.4a (rigid model), there is no methane between two cages in all concentration of guest molecules while in Figure 4.4b methane molecules can be found in the connecting area between the cages through six-membered rings. In this case methane molecules not only moved inside the cage but also diffused from one cage to other cages.

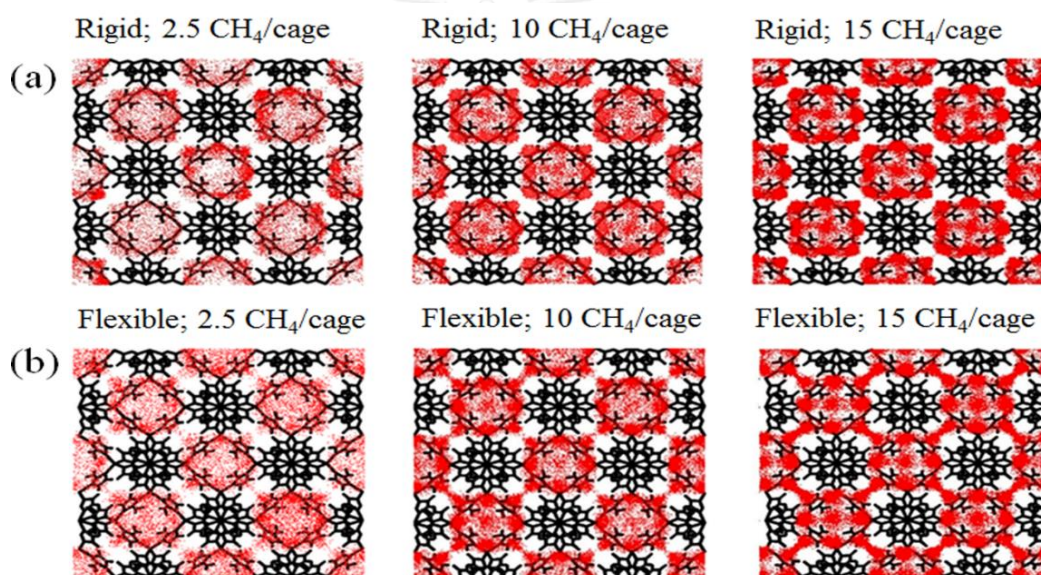


Figure 4.4. Probability density of CH<sub>4</sub> in (a) rigid model and (b) flexible model at 2.5, 10 and 15 CH<sub>4</sub> molecules/cage.

Figure 4.5 shows the RDFs between guest molecules with selected atom types of lattice and guest-guest interaction. The atom types in ZIF-90 were named in Figure S1 in the appendix. These RDFs were taken from the GEMC (MC\_rigid) at 1 bar, MD with flexible and rigid model at very low loading of 0.5 molecules/cage (1 bar) to compare with each other. For low loadings the interaction with the lattice dominates and thus it is a good test for the influence of the lattice flexibility. In Figure 4.5d, methane in

rigid model in MD cannot have the normal distribution because of the blockage of particle exchange between different cages. The random insertions and removals of guest molecules in GEMC leads to particle exchanges even if we assume the framework in GEMC to be rigid, so that the diffusion can also be found in GEMC as in flexible MD simulations. Figures 4.5a-c show the influence of the flexibility of the framework on the adsorption isotherm. In general, the RDFs from rigid MC show a better agreement with flexible MD than rigid MD.

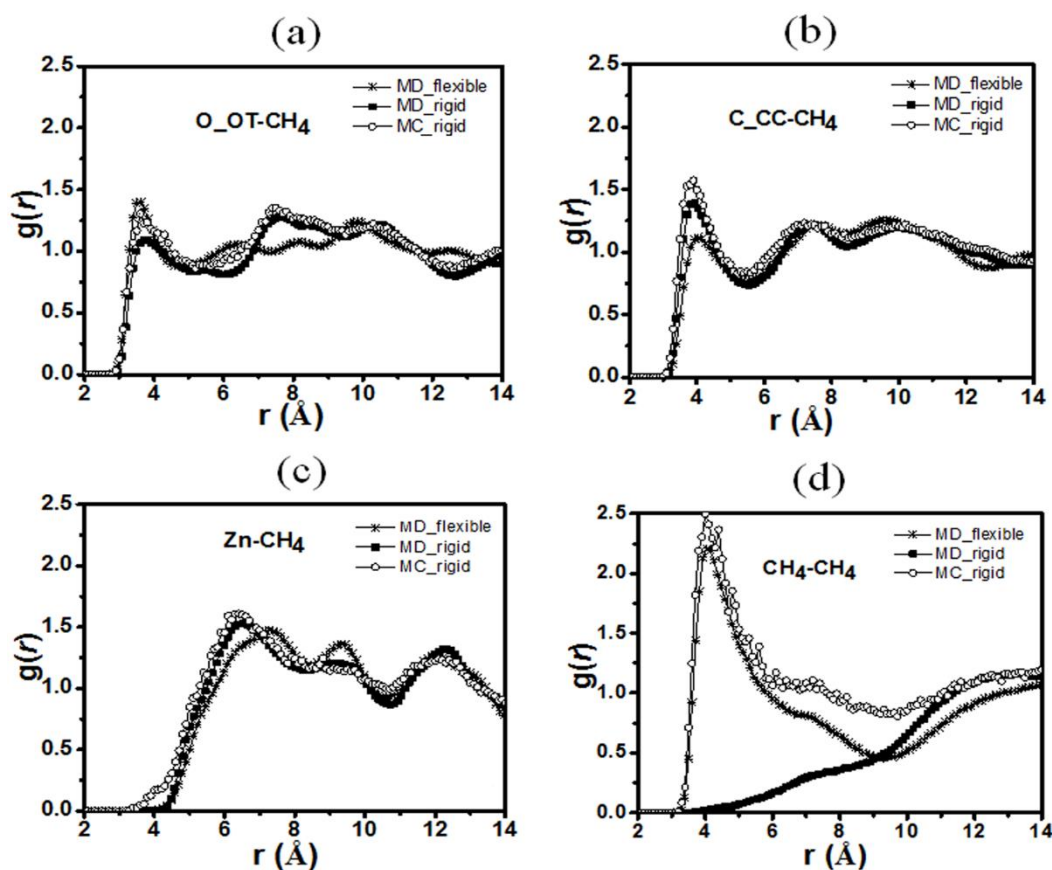


Figure 4.5. RDFs of the interaction between methane-methane and methane-ZIF-90 lattice in GEMC, rigid and flexible MD simulations at very low loading (0.5  $CH_4$  molecules/cage) with modified GAFF at 300 K.

To decide if the uptake in rigid lattice GEMC and flexible lattice MD at given pressure is equal, it would be necessary to measure the pressure in flexible lattice MD.

The pressure calculation *e.g.* using the virial theorem is ambiguous for porous solids for several reasons (as mentioned above) particularly in presence of partial charges and at high pressure. A more appropriate quantity to decide about the equilibrium between different systems in such cases is the chemical potential that must have the same value for each species in all parts of a system that are in equilibrium with each other. The chemical potential  $\mu$  can be obtained from the Gibbon program and from selected snapshots taken from the trajectory of an MD simulation by Widom's particle insertion method [11]. Using  $\mu$  instead of the pressure as the independent variable of state, the uptake is plotted in Figure 4.6. In the low concentration (low pressure) area, the results from GEMC and flexible MD are in quite good agreement. Slightly larger deviation appears only at high concentrations (high pressure). These results again support the possibility that an adsorption isotherm can be obtained from rigid lattice GEMC simulation.

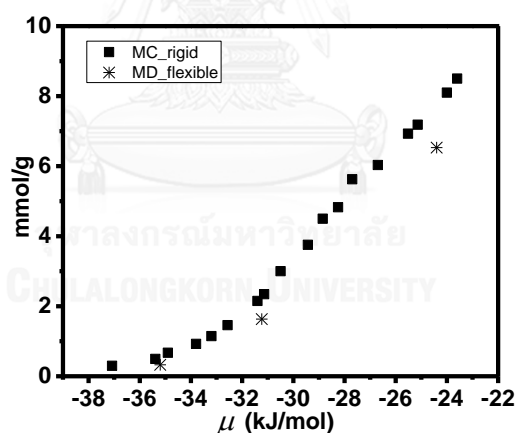


Figure 4.6. Uptake of  $\text{CH}_4$  by ZIF-90 at 300 K in mmol/g as a function of the chemical potential (kJ/mol) as obtained both from GEMC (MC\_rigid) and flexible MD.

#### 4.1.3. Adsorption sites

In numerous previous papers on MOFs and ZIFs it was found that sometimes the metal ion is the preferential site for adsorption like  $\text{H}_2$  in MOF-505 or  $\text{CO}_2$  in IRMOFs [56, 57]. In other ZIFs the organic linkers interact strongly with the guest molecules and

these became the preferential adsorption sites like for alcohol in ZIF-90, H<sub>2</sub> in various ZIFs or CH<sub>4</sub> in ZIF-3, 10 [21, 58, 59]. For a deeper understanding of the adsorption process, the adsorption site was studied.

The radial distribution functions (RDFs) between methane and selected atoms in the framework are plotted at very low (0.5 molecules/cage) and at very high (15 molecules/cage) loadings in MD simulation with modified GAFF force field. The RDFs between methane and all atom types are given in the appendix (Figure S4).

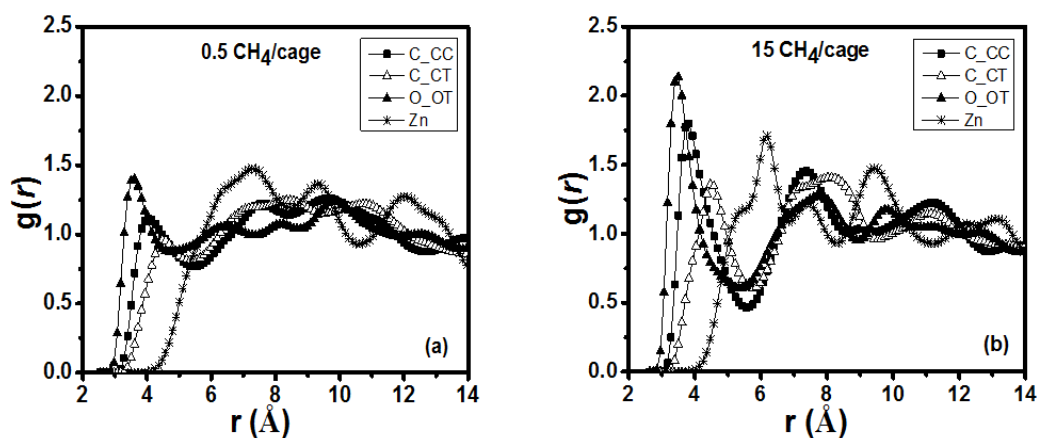


Figure 4.7. RDF of different atom types in ZIF-90 with CH<sub>4</sub> at loadings of a) 0.5 molecules/cage, b) 15 molecules/cage at 300 K.

At low loading (0.5 molecules/cage), the first RDF peak for Zn-CH<sub>4</sub> appeared at around 7.5 Å which was very large since the favorite distances between the metal ion (Zn) and the guest molecules (CH<sub>4</sub>, CO<sub>2</sub> and N<sub>2</sub>) in common ZIFs are around 2-4 Å [45]. Furthermore, the distances measured from CH<sub>4</sub> to O\_OT and C\_CC were found to be shorter (3.6 and 4 Å) than the distance between CH<sub>4</sub> and Zn. Thus, at low loading, methane molecules are preferentially located at the organic linker or - in other words - the preferential adsorption site is the organic linker. Among them, the first peak at O\_OT is the closest and highest one. It is not surprising that O\_OT is the most favorite site of methane based on the strong van der Waals interaction between O and CH<sub>4</sub>. The next peak belongs to C=C in the ring where the distance around CH<sub>4</sub> is about 4 Å.

This agrees with other work, in which the adsorption sites of alcohol with ZIF-90 are also C=O of the aldehyde group and C=C in the organic linker [5]. At very high loading, it is clear that the peaks became higher and the distances became closer, especially the favorite distance between Zn-CH<sub>4</sub> was shifted from 7.2 Å to around 6 Å. RDFs of C=O and C=C with CH<sub>4</sub> in different concentrations were also plotted in Figure S5 (appendix).

It should be noted that the density plots also visualize the positions of methane in ZIF-90, which is in accordance with the RDF results. Especially at lower loading, the high density area of the point cloud representing the density of methane was near at the organic linker at 2.5 methane molecules/cage. At higher loadings up to the concentration of 15 methane molecules/cage, the adsorption sites extended to the Zn metal ion. This corresponds to the closer peak of the RDF between Zn and methane in Figure 4.7.

As mentioned above the pressure at high loadings can be obtained from the Peng-Robinson equation of state applied to the gas phase in box A. At 15 molecules/cage the pressure is around 255 bar. Methane in the gas box of our simulation is still a gas at that pressure and temperature. It is difficult to reach such pressures in experiments but, such experimental investigations have been done already in some cases, e.g. in [60] measurements with ZIF-8 have been carried out at 14700 bar under loadings up to 41 methanol molecules per unit cell.

The adsorption isotherm from 0-255 bar from GEMC simulations with the modified force field GAFF can be seen in Figure 4.8. Bulk methane at 300 K has no gas-liquid phase transition. The adsorption isotherm is of Langmuir type and does not show any inflections.

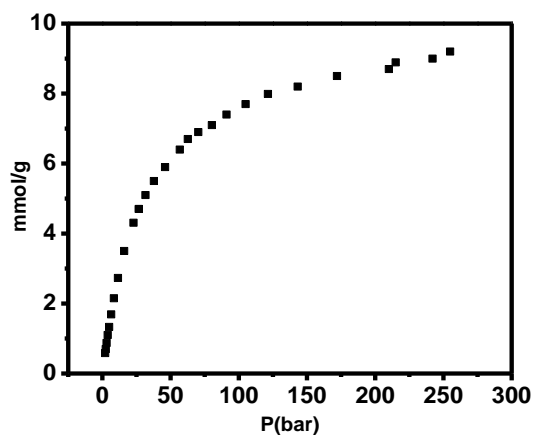


Figure 4.8. Adsorption isotherm of  $\text{CH}_4$  in ZIF-90 at 300 K for pressures 0-255 bar.

#### 4.1.4. Dynamical properties

The dynamical properties of guest molecules were examined by calculating their self-diffusion coefficient ( $D_s$ ). The dynamical behavior of the lattice was investigated by the window size distribution. These results have been obtained in NVE ensemble MD.

Based on the Einstein's relation,  $D_s$  can be calculated from the slope of the mean square displacement (MSD) as a function of the observation time. To examine the effect of framework flexibility to the diffusion, MD simulations were conducted on both rigid and flexible framework models. The MSD in the rigid and flexible framework are shown in Figure S3. The  $D_s$  data are given in Figure 4.10 and compared with the previous work of Atci et al. [10] who used a UFF rigid model for MD simulation. The  $D_s$  of methane was calculated to be zero in the DREID. 0.69 rigid model (see Figure S3) that means that no methane diffusion in ZIF-90 could be proven by this model.

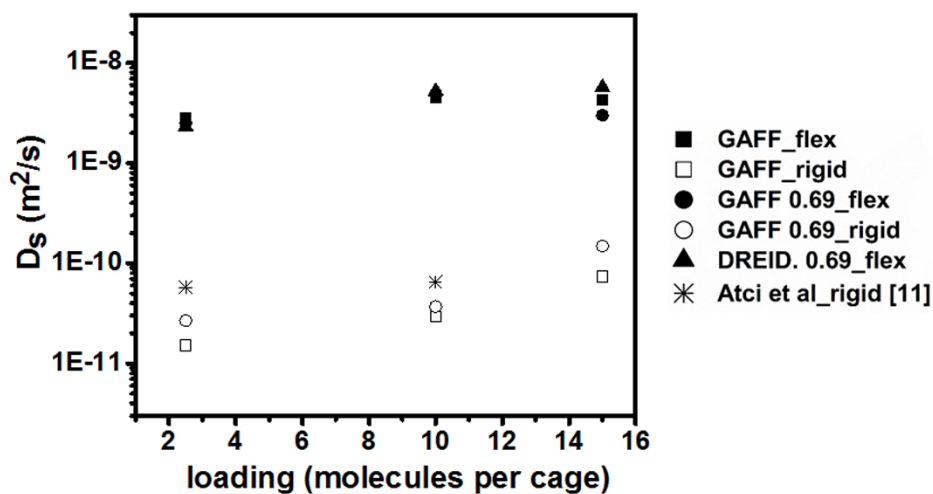


Figure 4.9. Comparison of  $D_s$  for  $\text{CH}_4$  in rigid and flexible ZIF-90 frameworks at 300 K.

In Figure 4.9 we can see the big gap of the  $D_s$  data between rigid and flexible framework. The methane can diffuse several orders of magnitude faster in the flexible model than in the rigid one. However results for  $D_s$ , from the flexible force fields, modified DREIDING, modified GAFF and original GAFF are similar. The larger average window diameter of DREIDING obviously compensates the influence of the lower flexibility for methane in ZIF-90 for this force field.

In Atci et al., the authors tried to compare their results with experimental permeation measurements. However, their predicted permeances for relative large molecules like methane, nitrogen were much lower than the experimental data. In [10] this was explained by the underestimation of  $D_s$  leading to a small permeance of these molecules. According to [10] the rigid framework was the reason. Therefore, to obtain a more suitable  $D_s$ , a flexible model is necessary. From the adsorption isotherm and  $D_s$  at 200°C and 1 bar with modified GAFF, the permeability was calculated by the below formula [11]. The permeance of methane through ZIF-90 obtained in this work is  $3.5 \times 10^{-8}$  ( $\text{mol.m}^{-2}.\text{s}^{-1}.\text{Pa}^{-1}$ ). This is twice the experimental value of Huang et al. [8] which is  $1.57 \times 10^{-8}$  ( $\text{mol.m}^{-2}.\text{s}^{-1}.\text{Pa}^{-1}$ ). Nevertheless, our value is nearer to the experiment than the value from rigid model in Atci et al. [10], which is  $3.0 \times 10^{-9}$  ( $\text{mol.m}^{-2}.\text{s}^{-1}.\text{Pa}^{-1}$ ). The remaining difference could be explained by imperfect crystals in



the real experiment while the crystal is considered ideal in the simulation. The detail of the calculation can be found in the appendix.

$$P_{ZIF} = \Pi_{ZIF} l = D_s \Phi \frac{c}{f} \quad (4.1)$$

in which,  $P$  is the permeability ( $\text{mol.m}^{-1}.\text{s}^{-1}.\text{Pa}^{-1}$ ),  $\Pi$  is the permeance ( $\text{mol.m}^{-2}.\text{s}^{-1}.\text{Pa}^{-1}$ ),  $l$  (m) is the top layer thickness with  $l = 20$  ( $\mu\text{m}$ ) [8],  $\Phi$  is helium void fraction (Widom Insertion method), in ZIF-90,  $\Phi = 0.498$  [11],  $c$  ( $\text{mol.m}^{-3}$ ) is equilibrium gas concentration,  $f$  (Pa) is the fugacity.

At different loadings of methane in ZIF-90, the average window size of ZIF-90 was nearly unchanged, it increases from 3.525 Å to 3.555 Å at 2.5  $\text{CH}_4/\text{cage}$  and decrease at very high loading from 3.555 Å to 3.495 Å (Figure 4.11).

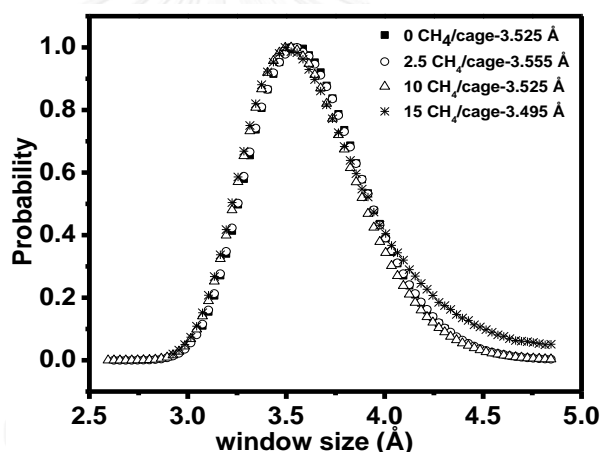


Figure 4.10. Distributions of the window size of ZIF-90 for different loadings of  $\text{CH}_4$  at 300 K.

Throughout the observed range of density and hence pressure up to 255 bar, no discontinuous change of the window size appears. This indicates that no structural change like gate opening [20, 61] can be observed and the experimentally observed adsorption and permeation of “too big methane” molecules is explained by the framework flexibility of ZIF-90.

## 4.2. Hydrogen

### 4.2.1. Adsorption and the preferential adsorption site of hydrogen and mixture in ZIF-90

The adsorption of hydrogen, methane and the mixture of  $\text{CH}_4/\text{H}_2$  with ratio 1:1 are collected in Figure 4.11 at low pressure (0-1.2 bar).

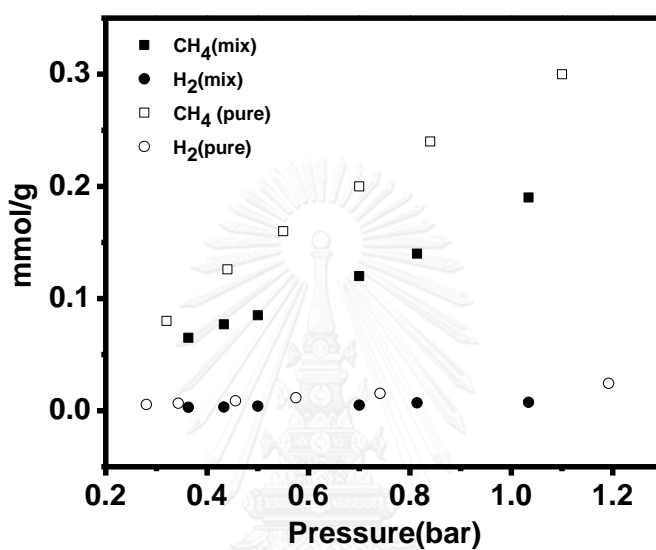


Figure 4.11. The adsorption isotherm of methane, hydrogen and mixture  $\text{CH}_4/\text{H}_2$  with the ratio 1:1

Hydrogen seems not likely to adsorb on ZIF-90, the amount of the adsorption of hydrogen in pure bulk gas as well as in mixture is negligible as seen in Figure 4.11.

In mixture, at the same pressure, the adsorbed methane in mixture on ZIF-90 is fewer than that of pure methane. From the different adsorption capability, the adsorption selectivities of mixture 1:1  $\text{CH}_4/\text{H}_2$  are around the range 14 to 16.

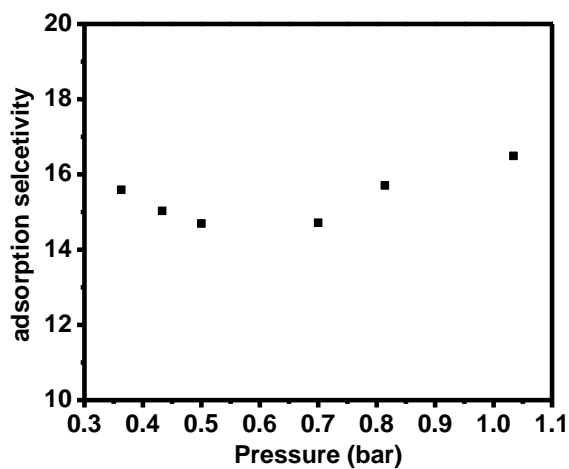


Figure 4.12. The adsorption selectivities of mixture  $\text{CH}_4/\text{H}_2$  with ratio 1:1

RDFs are plotted in Figure 4.13 to find the adsorption site of methane and hydrogen in the mixture.

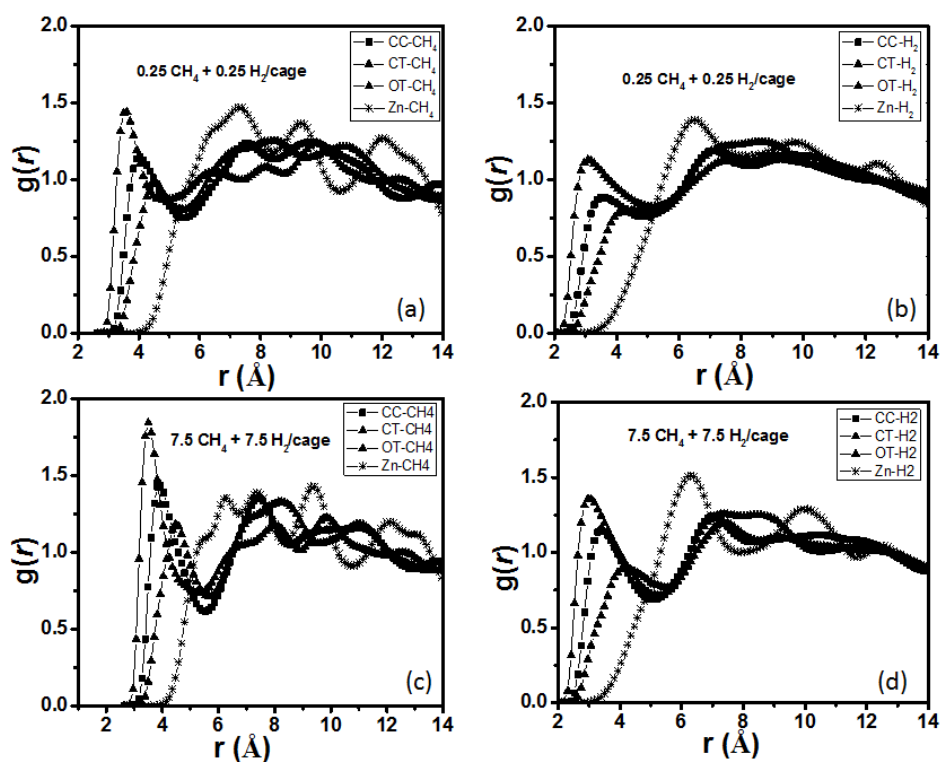


Figure 4.13. The RDFs of selected atom types in ZIF-90 with methane (a, c) and hydrogen (b, d) in two different concentrations.

There is no surprise that O<sub>OT</sub> is still the most favorable adsorption site in ZIF-90 of methane and hydrogen. The peak of RDFs in H<sub>2</sub> is also lower than in CH<sub>4</sub>, corresponding to the lower amount of adsorption.

Increasing the concentration, the first peaks of RDFs also enhances significantly in methane while in hydrogen, it increases slightly. Hence, the amount of H<sub>2</sub> that can adsorb on ZIF-90 is nearly unchanged upon to the pressure and also very few.

#### 4.2.2. Diffusion and membrane selectivity.

On the other hand, H<sub>2</sub> possesses a small diameter so that it diffuses very fast inside ZIF-90 (3.5 Å). Figure 4.14 shows the  $D_s$  of hydrogen and methane in both mixture and single bulk gas at many concentrations.

The different rate of the diffusion between methane and hydrogen is one of the factors that is used for gas separation in membranes.

In Huang et al [8], the separation factor was calculated from the permeance of two gases, it can be the multiplier of adsorption selectivity and the diffusion selectivity and is called membrane separation. At 1 bar, the membrane separation is figured out at 4.1 while the experimental data is around 7.

The reason comes from the overestimated the  $D_s$  of methane due to the perfect crystal in the simulation that mentioned above, it makes the diffusion selectivity lower than expected so that the separation factor is also lower than nearly twice when it is compared with the experiment. In general, ZIF-90 exhibits the high potential for the hydrogen purification not only at the room temperature but also at very high temperature (up to 225°C).

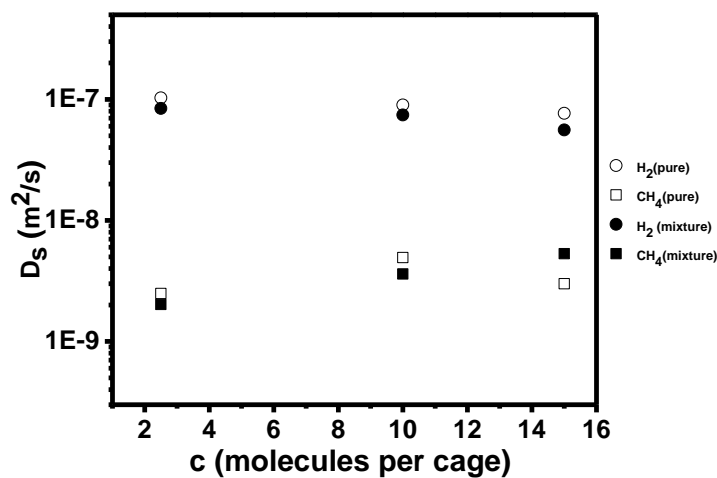


Figure 4.14. The self-diffusion coefficient of methane, hydrogen and mixture CH<sub>4</sub>/H<sub>2</sub> with the ratio 1:1

Similarly with the pure methane, no gate-opening effect occurs in the mixture CH<sub>4</sub>/H<sub>2</sub> at 300 K even at very high concentration. The window size of ZIF-90 still remains around 3.5 Å which fits very well with the experiment. The window size is gathered in Figure 4.15.

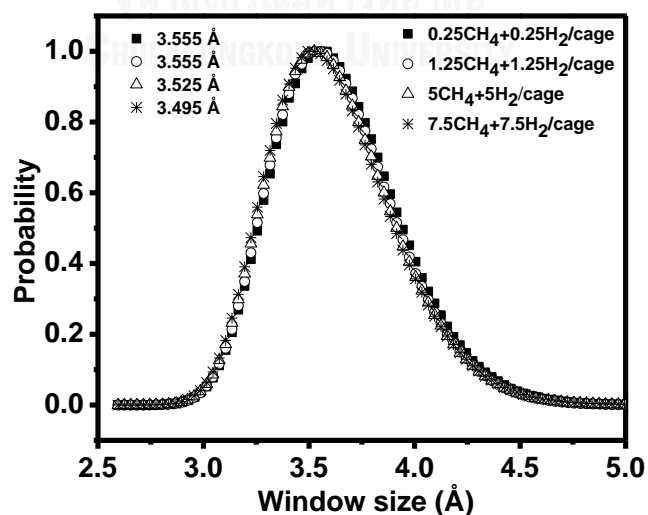


Figure 4.15. Distributions of the window size of ZIF-90 for different loadings of mixture CH<sub>4</sub>/H<sub>2</sub> with ratio 1:1 at 300 K.

In addition, the probability density of mixture  $\text{CH}_4/\text{H}_2$  were plotted in three concentrations (in figure 4.16).

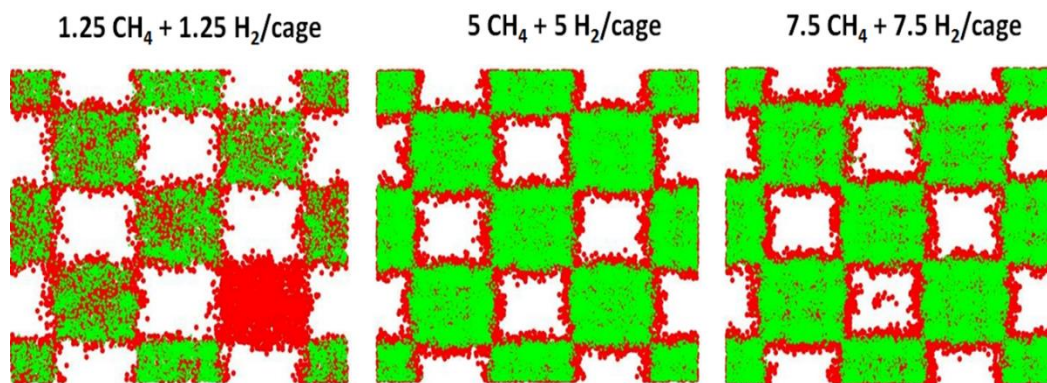
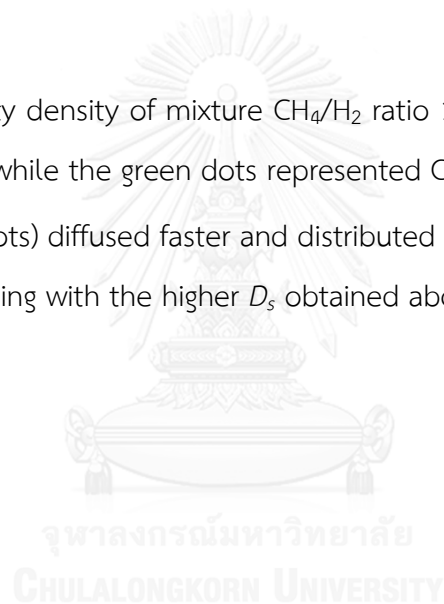


Figure 4.16. Probability density of mixture  $\text{CH}_4/\text{H}_2$  ratio 1:1 in flexible model. The red dots represented  $\text{H}_2$  while the green dots represented  $\text{CH}_4$ .

The  $\text{H}_2$  (red dots) diffused faster and distributed more equally than  $\text{CH}_4$  (green dots). It is corresponding with the higher  $D_s$  obtained above.



## CHAPTER V

### CONCLUSION

Among the tested force fields, the modified GAFF force field gave the best agreement of the simulated ZIF-90 structure (window size, and box length) and adsorption isotherms with the experiment. With this GAFF force field also the unit cell size could be reproduced in NPT simulations. The behavior of adsorbed guest molecules could be examined on a molecular scale. The flexibility of the framework affects significantly the self-diffusion coefficient ( $D_s$ ) of CH<sub>4</sub> in ZIF-90. The  $D_s$  obtained from flexible framework is between 1.5 to 2 orders of magnitude higher than  $D_s$  obtained for a rigid framework. The reason is that methane molecules can pass through the window in the flexible model. This was visualized by probability density plots and confirmed by the window size distribution.

Hydrogen is not likely to adsorb on the ZIF-90 but diffuses very fast inside it. In the mixtures, based on the difference of adsorption and diffusion rate, ZIF-90 shows a promising capability for membrane separation application. The separation factor obtained from the calculation is 4.1. It is lower than the experiment because of the overestimation of diffusion of methane due to the assumed perfect crystal in the simulations.

The window size is nearly independent upon the pressure. Hence, no structural change like gate opening has been observed for the methane and mixture methane/hydrogen in ZIF-90 system up to 255 bar.

The RDFs showed that the adsorption site for methane and hydrogen in ZIF-90 at low loading is mainly the organic linker. At higher loading, also the Zn ions become adsorption sites and also the cage centers and even the windows connecting adjacent cages show a reasonable probability for methane. An adsorption isotherm of methane from 0-255 bar could be obtained for which experimental data for the high pressures are still missing.

## REFERENCES

1. Batten S. R., C.N.R., Chen X. M., Garcia-Martinez J., Kitagawa S., Öhrström L., M.P. Suh, and J. Reedijk, *Terminology of Metal–Organic Frameworks and Coordination Polymers*. Pure and Applied Chemistry, 2013. **85**: p. 1715-1724.
2. Pimentel, B.R., Parulkar, A., Zhou, E., Brunelli, N. A., Lively, R. P., *Zeolitic Imidazolate Frameworks: Next-Generation Materials for Energy-Efficient Gas Separations*. ChemSusChem, 2014. **7**(12): p. 3202-3240.
3. Morris, W., Doonan, C. J., Furukawa, H., Banerjee, R., Yaghi, O. M., *Crystals as Molecules: Postsynthesis Covalent Functionalization of Zeolitic Imidazolate Frameworks*. Journal of the American Chemical Society, 2008. **130**(38): p. 12626-12627.
4. Raveendran, P., Y. Ikushima, and S.L. Wallen, *Polar Attributes of Supercritical Carbon Dioxide*. Accounts of Chemical Research, 2005. **38**(6): p. 478-485.
5. Gee, J.A., Chung, J., Nair, S., Sholl, D. S., *Adsorption and Diffusion of Small Alcohols in Zeolitic Imidazolate Frameworks ZIF-8 and ZIF-90*. The Journal of Physical Chemistry C, 2013. **117**(6): p. 3169-3176.
6. Brown, A.J., et al., *Continuous Polycrystalline Zeolitic Imidazolate Framework-90 Membranes on Polymeric Hollow Fibers*. Angewandte Chemie International Edition, 2012. **51**(42): p. 10615-10618.
7. Huang, A., Liu, Q., Wang, N. Caro, J., *Organosilica functionalized zeolitic imidazolate framework ZIF-90 membrane for CO<sub>2</sub>/CH<sub>4</sub> separation*. Microporous and Mesoporous Materials, 2014. **192**(0): p. 18-22.
8. Huang, A., W. Dou, and J. Caro, *Steam-Stable Zeolitic Imidazolate Framework ZIF-90 Membrane with Hydrogen Selectivity through Covalent Functionalization*. Journal of the American Chemical Society, 2010. **132**(44): p. 15562-15564.
9. Huang, A., N. Wang, and J. Kong C. and Caro, *Organosilica-Functionalized Zeolitic Imidazolate Framework ZIF-90 Membrane with High Gas-Separation Performance*. Angewandte Chemie 2012. **51**: p. 10551-10555.



10. Atci, E. and S. Keskin, *Understanding the Potential of Zeolite Imidazolate Framework Membranes in Gas Separations Using Atomically Detailed Calculations*. The Journal of Physical Chemistry C 2012. **116**(29): p. 15525–15537.
11. Thornton, A.W., Dubbeldam, D., Liu, M. S., Ladewig, B. P., Hill, A. J., Hill, M. R., *Feasibility of zeolitic imidazolate framework membranes for clean energy applications*. Energy & Environmental Science, 2012. **5**(6): p. 7637-7646.
12. Chokbunpiam, T., et al., *The importance of lattice flexibility for the migration of ethane in ZIF-8: Molecular dynamics simulations*. Microporous and Mesoporous Materials, 2013. **174**: p. 126-134.
13. Haldoupis, E., et al., *Quantifying Large Effects of Framework Flexibility on Diffusion in MOFs: CH<sub>4</sub> and CO<sub>2</sub> in ZIF-8*. ChemPhysChem, 2012. **13**(15): p. 3449-3452.
14. Hertäg, L., et al., *Diffusion of CH<sub>4</sub> and H<sub>2</sub> in ZIF-8*. Journal of Membrane Science, 2011. **377**(1–2): p. 36-41.
15. Seehamart, K., et al., *Investigating the reasons for the significant influence of lattice flexibility on self-diffusivity of ethane in Zn(tbip)*. Microporous and Mesoporous Materials, 2010. **130**(1–3): p. 92-96.
16. Schierz, P., et al., *MD simulations of hydrogen diffusion in ZIF-11 with a force field fitted to experimental adsorption data*. Microporous and Mesoporous Materials, 2015. **203**: p. 132-138.
17. Zhang, L., G. Wu, and J. Jiang, *Adsorption and Diffusion of CO<sub>2</sub> and CH<sub>4</sub> in Zeolitic Imidazolate Framework-8: Effect of Structural Flexibility*. The Journal of Physical Chemistry C, 2014. **118**(17): p. 8788-8794.
18. Chokbunpiam, T., et al., *Gate opening effect for carbon dioxide in ZIF-8 by molecular dynamics – Confirmed, but at high CO<sub>2</sub> pressure*. Chemical Physics Letters, 2016. **648**: p. 178-181.
19. Gücüyener, C., et al., *Ethane/Ethene Separation Turned on Its Head: Selective Ethane Adsorption on the Metal–Organic Framework ZIF-7 through a Gate-Opening Mechanism*. Journal of the American Chemical Society, 2010. **132**(50): p. 17704-17706.

20. Zhang, L., Z. Hu, and J. Jiang, *Sorption-Induced Structural Transition of Zeolitic Imidazolate Framework-8: A Hybrid Molecular Simulation Study*. Journal of the American Chemical Society, 2013. **135**(9): p. 3722-3728.
21. Zhang, K., Nalaparaju, A., Chen, Y., Jiang, J., *Biofuel purification in zeolitic imidazolate frameworks: the significant role of functional groups*. Physical Chemistry Chemical Physics, 2014. **16**(20): p. 9643-9655.
22. Park, K.S., et al., *Exceptional chemical and thermal stability of zeolitic imidazolate frameworks*. Proceedings of the National Academy of Sciences, 2006. **103**(27): p. 10186-10191.
23. Chen, B., et al., *Zeolitic imidazolate framework materials: recent progress in synthesis and applications*. Journal of Materials Chemistry A, 2014. **2**(40): p. 16811-16831.
24. Jiang, H.-L., et al., *Au@ZIF-8: CO Oxidation over Gold Nanoparticles Deposited to Metal–Organic Framework*. Journal of the American Chemical Society, 2009. **131**(32): p. 11302-11303.
25. Fang, J., et al., *Extremely low frequency alternating magnetic field-triggered and MRI-traced drug delivery by optimized magnetic zeolitic imidazolate framework-90 nanoparticles*. Nanoscale, 2016. **8**(6): p. 3259-3263.
26. Jones, C.G., et al., *Versatile Synthesis and Fluorescent Labeling of ZIF-90 Nanoparticles for Biomedical Applications*. ACS Applied Materials & Interfaces, 2016. **8**(12): p. 7623-7630.
27. Liu, C. and B. Yan, *Luminescent zinc metal-organic framework (ZIF-90) for sensing metal ions, anions and small molecules*. Photochemical & Photobiological Sciences, 2015. **14**(9): p. 1644-1650.
28. Thompson, J.A., et al., *Tunable CO<sub>2</sub> Adsorbents by Mixed-Linker Synthesis and Postsynthetic Modification of Zeolitic Imidazolate Frameworks*. The Journal of Physical Chemistry C, 2013. **117**(16): p. 8198-8207.
29. Huang, A. and J. Caro, *Covalent Post-Functionalization of Zeolitic Imidazolate Framework ZIF-90 Membrane for Enhanced Hydrogen Selectivity*. Angewandte Chemie 2011. **50**: p. 4979-4982.

30. Amrouche, H., Aguado, S., Pérez-Pellitero, J., Chizallet, C., Siperstein, F., Farrusseng, D., N. Bats, and C. Nieto-Draghi, *Experimental and Computational Study of Functionality Impact on Sodalite–Zeolitic Imidazolate Frameworks for CO<sub>2</sub> Separation*. *The Journal of Physical Chemistry C*, 2011. **115**(33): p. 16425-16432.
31. Venkatasubramanian, A., Navaei, M., Bagnall, K. R., McCarley, K. C., Nair, S., Hesketh, P. J., *Gas Adsorption Characteristics of Metal–Organic Frameworks via Quartz Crystal Microbalance Techniques*. *The Journal of Physical Chemistry C*, 2012. **116**(29): p. 15313-15321.
32. Diestel, L., Wang, N., Schulz, A., Steinbach, F., Caro, J., *Matrimid-Based Mixed Matrix Membranes: Interpretation and Correlation of Experimental Findings for Zeolitic Imidazolate Frameworks as Fillers in H<sub>2</sub>/CO<sub>2</sub> Separation*. *Industrial & Engineering Chemistry Research*, 2015. **54**(3): p. 1103-1112.
33. Yilmaz, G. and S. Keskin, *Molecular modeling of MOF and ZIF-filled MMMs for CO<sub>2</sub>/N<sub>2</sub> separations*. *Journal of Membrane Science*, 2014. **454**(0): p. 407-417.
34. Chandler, D., *Introduction to Modern Statistical Mechanics*. Oxford University Press, 1987.
35. Leach, A.R., *Molecular modelling: Principles and applications*, E.P.E. Limited, Editor. 2001.
36. Thomas Engel, P.J.R., *Thermodynamics, Statistical Thermodynamics, & Kinetics*. Prentice Hall 2009. **second edition**: p. 327.
37. Gibbs, J.W., *Elementary Principles in Statistical Mechanics*. New York: Charles Scribner's Sons, 1902.
38. Athanassios, Z.P., *Monte Carlo methods for phase equilibria of fluids*. *Journal of Physics: Condensed Matter*, 2000. **12**(3): p. R25.
39. Salonen, E., *Introduction to Molecular Dynamics Simulations*. Ruhr-University Bochum 23.-27.10.2006.
40. Fritzsche, S., *Simple and Advanced Technics of Molecular-Dynamics-Simulations (MD)*, F.o.P.a.G. University of Leipzig, Institute of Theoretical Physics., Editor. 2015. p. 12.

41. Baker, R.W., *Membrane technology*. Kirk Othmer Encyclopedia of Chemical Technology. Vol. 16. 1995, Singapore: Wiley.
42. Gavalas, G.R., *Diffusion in Microporous Membranes: Measurements and Modeling*. Ind. Eng. Chem. Res. , 2008. **47**,.
43. Krishna, R., *Describing the Diffusion of Guest Molecules Inside Porous Structures*. J. Phys. Chem. C, 2009,. **113**, .
44. A. Fick, *Ueber Diffusion*. Pogg. Ann. Phys. Chem. , 1855. **170**: p. 59-86.
45. Pérez-Pellitero, J., et al., *Adsorption of CO<sub>2</sub>, CH<sub>4</sub>, and N<sub>2</sub> on Zeolitic Imidazolate Frameworks: Experiments and Simulations*. Chemistry – A European Journal, 2010. **16**(5): p. 1560-1571.
46. García-Pérez, E., et al., *A computational study of CO<sub>2</sub>, N<sub>2</sub>, and CH<sub>4</sub> adsorption in zeolites*. Adsorption, 2007. **13**(5-6): p. 469-476.
47. Prakash, M., N. Sakhavand, and R. Shahsavari, *H<sub>2</sub>, N<sub>2</sub>, and CH<sub>4</sub> Gas Adsorption in Zeolitic Imidazolate Framework-95 and -100: Ab Initio Based Grand Canonical Monte Carlo Simulations*. The Journal of Physical Chemistry C, 2013. **117**(46): p. 24407-24416.
48. Mendoza-Cortés, J.L., et al., *Adsorption Mechanism and Uptake of Methane in Covalent Organic Frameworks: Theory and Experiment*. The Journal of Physical Chemistry A, 2010. **114**(40): p. 10824-10833.
49. Costantini, A. and A. Laganà, *Investigation of Propane and Methane Bulk Properties Structure Using Two Different Force Fields*, in *Computational Science and Its Applications – ICCSA 2008*, O. Gervasi, et al., Editors. 2008, Springer Berlin Heidelberg. p. 1052-1064.
50. Rull, L.F., G. Jackson, and B. Smit, *The condition of microscopic reversibility in Gibbs ensemble Monte Carlo simulations of phase equilibria*. Molecular Physics, 1995. **85**(3): p. 435-447.
51. Koblinski, P., et al., *Molecular dynamics study of screening in ionic fluids*. The Journal of Chemical Physics, 2000. **113**(1): p. 282-291.
52. Hansen, J.S., T.B. Schrøder, and J.C. Dyre, *Simplistic Coulomb Forces in Molecular Dynamics: Comparing the Wolf and Shifted-Force Approximations*. The Journal of Physical Chemistry B, 2012. **116**(19): p. 5738-5743.

53. Peng, D.Y., and Robinson, D. B., *A New Two-Constant Equation of State*. Industrial and Engineering Chemistry: Fundamentals, 1976. **15**: p. 59–64.
54. [http://www.csar.cfs.ac.uk/user\\_information/software/chemistry/](http://www.csar.cfs.ac.uk/user_information/software/chemistry/).
55. Zhang, C., et al., *Unexpected Molecular Sieving Properties of Zeolitic Imidazolate Framework-8*. The Journal of Physical Chemistry Letters, 2012. **3**(16): p. 2130-2134.
56. Babarao, R. and J. Jiang, *Molecular Screening of Metal–Organic Frameworks for CO<sub>2</sub> Storage*. Langmuir, 2008. **24**(12): p. 6270-6278.
57. Yang, Q. and C. Zhong, *Understanding Hydrogen Adsorption in Metal–Organic Frameworks with Open Metal Sites: A Computational Study*. The Journal of Physical Chemistry B, 2006. **110**(2): p. 655-658.
58. Assfour, B., et al., *Hydrogen storage in zeolite imidazolate frameworks. A multiscale theoretical investigation*. International Journal of Hydrogen Energy, 2011. **36**(10): p. 6005-6013.
59. Guo, H.-c., et al., *Molecular Simulation for Adsorption and Separation of CH<sub>4</sub>/H<sub>2</sub> in Zeolitic Imidazolate Frameworks*. The Journal of Physical Chemistry C, 2010. **114**(28): p. 12158-12165.
60. Moggach, S.A., T.D. Bennett, and A.K. Cheetham, *The Effect of Pressure on ZIF-8: Increasing Pore Size with Pressure and the Formation of a High-Pressure Phase at 1.47 GPa*. Angewandte Chemie, 2009. **121**(38): p. 7221-7223.
61. Chokbunpiam, T., et al., *N<sub>2</sub> in ZIF-8: Sorbate induced structural changes and self-diffusion*. Microporous and Mesoporous Materials, 2014. **187**: p. 1-6.

## ภาคผนวก

### Cutoff treatment for small neutral molecules

First it has been shown that in many particle systems, which are neutral in sum of the charges, for large distances Coulomb interactions are reduced by many-particle effects and can be dropped down by shifted forces or similar models instead to use computer time expensive methods like Ewald summation.

We made tests that showed that for small molecules the efficiency of this method can be strongly improved by a simple trick: The Coulomb interaction between two isolated partial charges  $i$  and  $l$  (belonging to atoms of guest molecules or, to lattice atoms, respectively)

$$U_{il}(r_{il}) = \frac{q_i q_l}{4\pi\epsilon_0 r_{il}} \quad r_{il} = |\vec{r}_i - \vec{r}_l| \quad (1)$$

can be several kJ/mol even at 30 Å. But each guest molecule is neutral in the sum of its partial charges. Therefore, the sum of all Coulomb interactions  $i=1, \dots, N_A$

$$U_{Al} = \sum_{i=1}^{N_A} U_{il}(r_{il}) \quad (2)$$

of one given guest molecule (named A) with another given charge (here called  $l$ ) anywhere in the system at far distance at is normally orders of magnitude smaller than the single summands of this sum. This makes sense because for molecules, for which charge and dipole moment are zero in sum (valid for all molecules in this work), only faster decaying quadrupole moments and higher multipole moments will remain at large distances.

For illustration let us consider a CO<sub>2</sub> molecule directed along the x-axis with the C atom in the origin. Let the partial charges of each oxygen be -0.294e and let that of the C be 0.588e. Let us consider the interaction with a fictive Zn atom as it could exist in the lattice. Let the Zn have a partial charge of 1.174e. The net Coulomb interaction between the molecule and the Zn has its largest amount, if the position of the Zn is on the x-axis because the differences in the distances from the Zn to the atoms of CO<sub>2</sub> are then mostly significant. The Coulomb interaction of the C atom with the Zn that is at the position  $x = 30$  Å is still 32 kJ/mol, but the sum of all three Coulomb

interactions including also the oxygen atoms is only -0.048 kJ/mol. For all other positions (not on the x-axis) of the Zn at a distance of 30 Å from the origin this sum will be even smaller.

Note, that the different positions of the partial charges of molecule A (CO<sub>2</sub> in the example) will also lead to non-simultaneous cutoffs, if the cutoff is done separately for each partial charge of CO<sub>2</sub>. This will destroy the convenient balance in the sum.

Hence, cutoff errors will be smaller if the complete sum is cut off (or dropped down by a damping factor) at once, rather than cutting or damping the single pair interactions one by one. In detail this means the following:

Instead of a cutoff we use a damping factor  $\gamma(r)$  that is equal to one for  $r < r_a$ .

In  $r_a < r < r_b$  it is

$$\gamma(r) = \xi^2 (\xi^2 - 2) + 1 \quad \xi = (r - r_a) / (r_b - r_a) \quad (3)$$

And for  $r > r_b$   $\gamma(r)$  is zero. We have chosen  $r_a = 25$  Å and  $r_b = 30$  Å. The first derivative of  $\gamma(r)$  is zero at  $r_a$  and  $r_b$  enabling smooth curves even if forces are not needed in GEMC.

Damping the single pair interactions one by one would mean that a damped potential  $U_d$  that is used instead of the full potential would be defined by

$$U_{dAl} = \sum_{i=1}^{N_A} U_{il}(r_{il}) \gamma(r_{il}) \quad (4)$$

We propose better to use

$$U_{dAl} = \gamma(|\vec{r}_s - \vec{r}_l|) \sum_{i=1}^{N_A} U_{il}(r_{il}) \quad (5)$$

where  $\vec{r}_s$  is the site of the center of mass of the molecule A.

Of course this trick makes sense only if the size of the neutral molecule A is small in comparison to  $r_a$  and  $r_b$ . For large molecules parts of the molecule could be closer to  $l$  even if the center of mass of A is far away from  $l$ .

Table: Non-bonded interaction force field of ZIF-90 after scaling with GAFF, DREIDING

| # | Atom type | GAFF(scaling 0.69)    |              | DREIDING(scaling 0.69) |              |
|---|-----------|-----------------------|--------------|------------------------|--------------|
|   |           | $\epsilon$ (kcal/mol) | $\sigma$ (Å) | $\epsilon$ (kcal/mol)  | $\sigma$ (Å) |
| 1 | C_CR      | 0.059                 | 3.40         | 0.065                  | 3.47         |
| 2 | C_CC      | 0.059                 | 3.40         | 0.065                  | 3.47         |
| 3 | C_CT      | 0.059                 | 3.40         | 0.065                  | 3.47         |
| 4 | H_H4      | 0.010                 | 2.51         | 0.010                  | 2.85         |
| 5 | H_HT      | 0.010                 | 2.65         | 0.010                  | 2.85         |
| 6 | Zn        | 0.009                 | 1.96         | 0.037                  | 4.05         |
| 7 | O         | 0.140                 | 2.96         | 0.066                  | 3.03         |
| 8 | N         | 0.110                 | 3.25         | 0.050                  | 3.26         |

| # | Atom type | GAFF(scaling 0.54)    |              | DREIDING(scaling 0.54) |              |
|---|-----------|-----------------------|--------------|------------------------|--------------|
|   |           | $\epsilon$ (kcal/mol) | $\sigma$ (Å) | $\epsilon$ (kcal/mol)  | $\sigma$ (Å) |
| 1 | C_CR      | 0.046                 | 3.40         | 0.050                  | 3.47         |
| 2 | C_CC      | 0.046                 | 3.40         | 0.050                  | 3.47         |
| 3 | C_CT      | 0.046                 | 3.40         | 0.050                  | 3.47         |
| 4 | H_H4      | 0.008                 | 2.51         | 0.008                  | 2.85         |
| 5 | H_HT      | 0.008                 | 2.65         | 0.008                  | 2.85         |
| 6 | Zn        | 0.007                 | 1.96         | 0.029                  | 4.05         |
| 7 | O_OT      | 0.100                 | 2.96         | 0.050                  | 3.03         |
| 8 | N_NA      | 0.086                 | 3.25         | 0.040                  | 3.26         |



Figure S1. Organic linker in ZIF-90

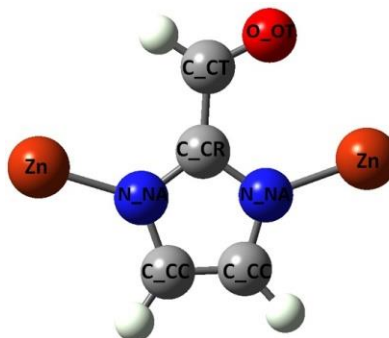


Figure S2: Distributions of box length obtained from NPT ensemble

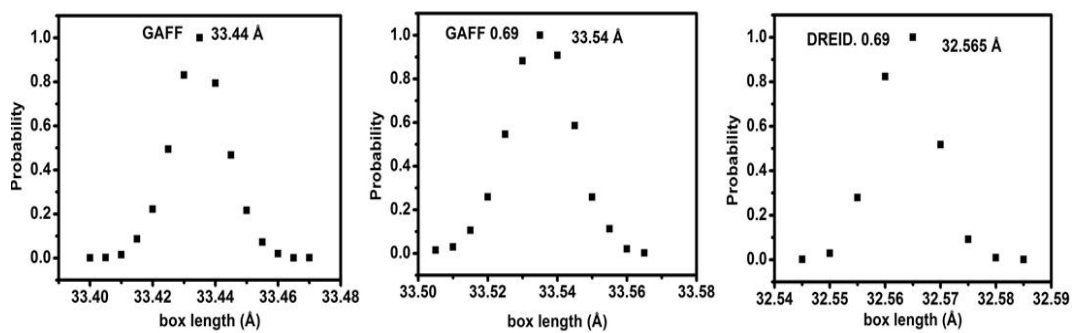


Figure S3. Some MSDs of CH<sub>4</sub> in ZIF-90 framework: a) rigid DREID. 0.69 in 2.5, 10, 15 molecules/cage (no diffusion), b) rigid GAFF and rigid GAFF 0.69 with normal diffusion at 2.5 molecules/cage, c) flexible GAFF and flexible GAFF 0.69 at 2.5 molecules/cage

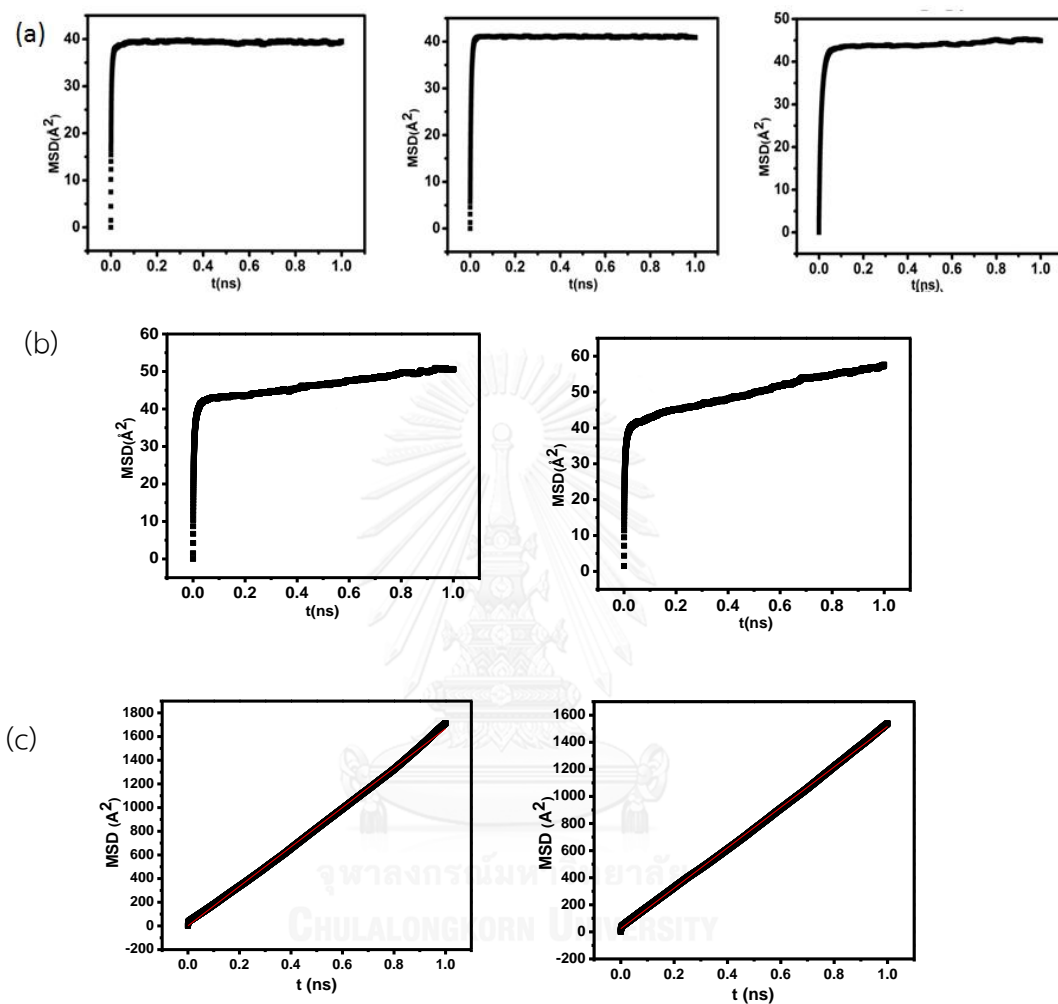


Figure S4. RDFs of all atom types in ZIF-90 with methane at 0.5 molecules/cage and 15 molecules/cage using flexible framework with modified GAFF in MD simulation.

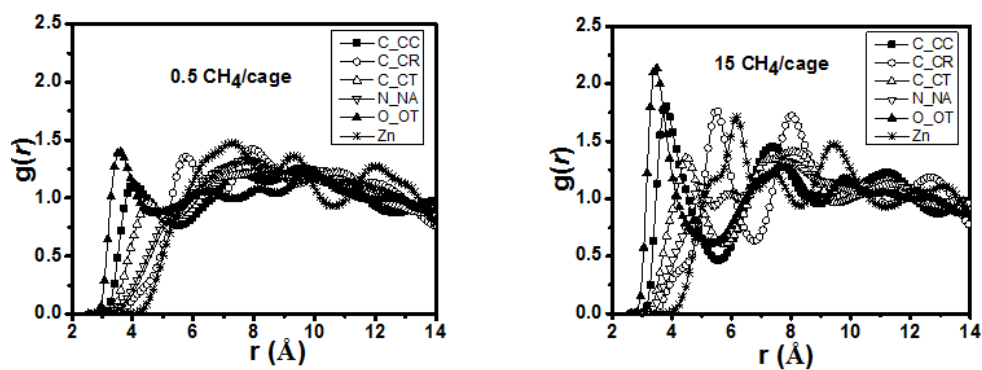
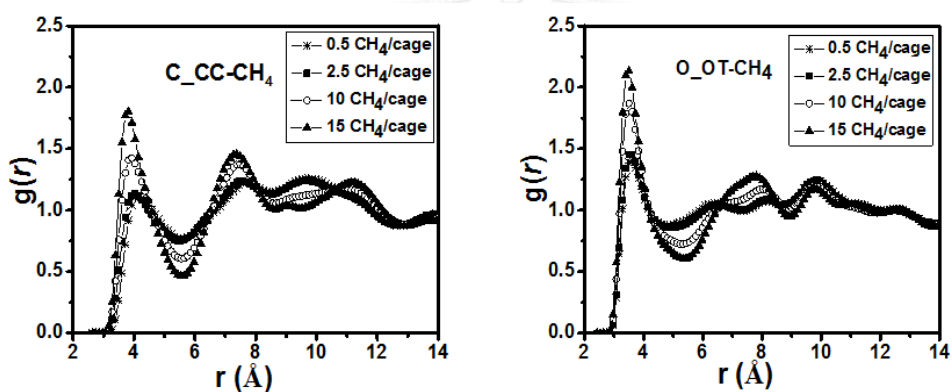


Figure S5. RDFs of C=C (C\_CC) and O (O\_OT) with CH<sub>4</sub> at various concentrations using flexible framework with modified GAFF in MD simulation.



Calculation permeance from the amount of adsorption and  $D_s$

$$\Pi_{ZIF} = D_s \Phi \frac{c}{f * l}$$

$D_s$ : self-diffusion coefficient ( $m^2/s$ )

$\Phi$  is the void fraction=0.498

$c$ : equilibrium gas concentration ( $mol/m^3$ )

$f$ : fugacity (Pa)=pressure

$\Pi$ : permeance ( $mol.m^{-2}.s^{-1}.Pa^{-1}$ )

$l$ : top layer thickness (m) = 20  $\mu m$

- Convert from mmol/g to  $mol/m^3$

Density in ZIF-90 =  $M/(N_A * V) = 987602.317 g/m^3$

\* $M$ : molecular weight of 8 unit cells,  $M=24517.44$

\* $N_A$ : Avogadro number,  $N=6.023*10^{23}$

\* $V$ : volume of 8 unit cells,  $V = (34.543*10^{-10})^3 (m^3)$

$c(mol/m^3) = \text{adsorption (mmol/gam)} * \text{density (g/m}^3) * 10^{-3} (mol/mmol) = \text{adsorption}$

\* 987.602

$\rightarrow \Pi_{ZIF} (mol.m^{-1}.s^{-1}.Pa^{-1}) = D_s * 0.498 * \text{adsorption} * 987.602 / (20 * 10^{-6} * 101325)$

$D_s$  and amount of adsorption of methane are evaluated at 200°C and 1 bar.

$D_s = 3.73 \times 10^{-9} (m^2/s)$

Adsorption = 0.039 (mmol/g)

$\Pi_{ZIF} = 3.5 \times 10^{-8} (mol.m^{-2}.s^{-1}.Pa^{-1})$ .

## VITA

Name: Phuong Thuy Vo

Date of birth: June 4th, 1991

Place of birth: Binh Dinh – Vietnam

Foreign Language: IELTS 6.5 (each subject  $\geq 6.0$ )

Email: thuyphuonggnu@gmail.com

### Education

2006 – 2009: Pupil of Le Quy Don specialized high school

2009 – 2013: Bachelor of Chemistry at Faculty of Chemistry, Quy Nhon University, Vietnam (GPA=8.46/10, second class honor).

2014 - present: M.Sc., Department of Chemistry, Faculty of Science, Chulalongkorn University. (Final examination in June 2016)

### Scholarship

2014-2016: ASEAN scholarship option II, Graduate School, Chulalongkorn University.

### Publications

Vo Thuy Phuong, Nguyen Thi Thu Trang, Vien Vo, Nguyen Tien Trung, A Comparable Study of Interaction Capacity of CO<sub>2</sub> with the S=O and S=S groups in some doubly methylated and halogenated derivatives of CH<sub>3</sub>SOCH<sub>3</sub> and CH<sub>3</sub>SSCH<sub>3</sub> Chemical Physics Letters 2014, 598C, pp. 75-80.

Vo Thuy Phuong, T. Chokbunpiam\*, S. Fritzsche, T. Remsungnen, T.Rungrotmongkol, C. Chmelik, J. Caro, and S. Hannongbua\*, Methane in Zeolitic Imidazolate Framework ZIF-90: Adsorption and Diffusion by Molecular Dynamics and Gibbs Ensemble Monte Carlo, Microporous and Mesoporous Materials 2016, doi: 10.1016/j.micromeso.2016.06.029.